

Density-Graded Cellular Solids: Mechanics, Fabrication, and Applications

Oyindamola Rahman, Kazi Zahir Uddin, Jeeva Muthulingam, George Youssef, Chen Shen,* and Behrad Koohbor*

Cellular solids have gained extensive popularity in different areas of engineering due to their unique physical and mechanical properties. Recent advancements in manufacturing technologies have led to the development of cellular solids with highly controllable microstructures and properties modulated for multiple functionalities at low structural weights. The concept of density gradation in cellular solids has recently gained attention due to its potentials in opening new doors to the development of lightweight structures that offer optimal physical and mechanical properties without compromising their favorable characteristics. Herein, a comprehensive insight into the fundamental concepts, fabrication, and current and potential applications of density-graded cellular solids in various areas of science and engineering is provided. Cellular solids are broadly classified into two main categories: foams and lattice structures. An overview of the fundamental concepts in each category is presented, followed by details on the characterization approaches and some of the most novel processing techniques utilized in fabricating the structures. The uses of density-graded structures in load-bearing, acoustic, and biomedical applications are highlighted. The state of the art in each category and the current trends in application-specific optimization of density-graded structures are discussed. The review concludes with an outlook of the future directions in this exciting field.

insulation, tailorable specific strength, superior impact energy absorption, and cushioning performance, all at low structural weights. The tailorability of the macroscopic (bulk) behavior of these structures by tuning the base material properties and cellular architecture has led to the widespread applications of cellular solids in automotive, aerospace, sports, biomechanics, and packaging industries. It is established that density, load bearing, energy absorption, acoustic, and thermal properties of cellular solids are strongly dependent on the geometry, connectivity, and architecture of their cell structure. The property–structure–performance interdependence in cellular solids has led to the development of various types of stochastic or nonordered (foams) and periodic or ordered (lattices) structures with tailorable and application-specific properties. However, from a practical perspective, a common drawback in the design and development of cellular solids, especially for applications wherein the structure's load-bearing capacity is key, is the trade-off between specific strength and energy absorption properties.^[1] It has

1. Introduction


Cellular solids have found applications in numerous fields due to the combination of favorable properties, such as excellent thermal

been shown that increasing the cell-wall thickness in cellular solids generally leads to higher strength and lower energy absorption capacities. In contrast, specific energy absorption (strain energy absorbed normalized by weight) can be improved by reducing the cell-wall thickness at the cost of strength and stiffness.

O. Rahman, K. Z. Uddin, J. Muthulingam, C. Shen, B. Koohbor
Department of Mechanical Engineering
Rowan University
201 Mullica Hill Rd., Glassboro, NJ 08028, USA
E-mail: shenc@rowan.edu; koohbor@rowan.edu

G. Youssef
Experimental Mechanics Laboratory
Department of Mechanical Engineering
San Diego State University
5500 Campanile Drive, San Diego, CA 92182, USA

B. Koohbor
Advanced Materials & Manufacturing Institute
Rowan University
Glassboro, NJ 08028, USA

 The ORCID identification number(s) for the author(s) of this article can be found under <https://doi.org/10.1002/adem.202100646>.

DOI: 10.1002/adem.202100646

There have been major developments to address the strength–energy absorption dichotomy in cellular solids. For instance, the development of auxetic structures has opened doors to a new class of cellular structures that outperform their conventional counterparts in terms of improvements in resistance to deformation and indentation, increased load bearing and fracture resistance, and enhanced impact energy mitigating properties.^[2–4] Auxetic structures have proven promising, especially in sports applications as lightweight protective paddings with tunable properties.^[5] However, despite their potential in providing a pathway to achieving improved strength and cushioning performance, some difficulties need to be overcome and call for further development in this area. For example, the processing and fabrication of auxetic structures, especially auxetic foams, are not feasible for all polymer systems and require precise and often costly processing techniques.^[2,6]

Density gradation has recently been proposed as a promising approach that facilitates the development of lightweight, high strength, and high energy-absorbing cellular solids. Conceptually, density-graded cellular solids hinge on developing an integrated structure in which the local density is varied spatially and along specific directions, where the overall weight of the structure remains low, whereas its strength and energy absorption capacity (as well as other properties, e.g., acoustic, thermal insulation, etc.) are enhanced. Recent achievements in the development of density-graded structures point to the fact that density gradation can indeed improve the energy absorption of foams and lattice structures, while simultaneously enabling the tailorability of structural weight, load-bearing performance, and other functionalities. As such, there has been an increased interest in the design, fabrication, and characterization of density-graded cellular solids.

The present article attempts to provide an overview of the recent developments in the characterization, design and development, and applications of novel density-graded cellular solids, mainly from a solid mechanics perspective (see **Figure 1**). It should be emphasized that the present overview focuses on a new class of graded cellular structures, wherein the overall properties depend primarily on the spatial variation of density. As such, the present article focuses on a very specific class of functionally graded cellular solids. More fundamental discussions on the general topic of functionally graded structures can be found in a number of previously published studies.^[7,8] In the forthcoming sections, we first broadly categorize the two classes of structures, wherein density gradation has proven promising. These two categories are foams and lattices. **Section 2** highlights the mechanical characterization approaches utilized in the study of density-graded foams and lattice structures. An overview of the design and fabrication of density-graded cellular structures, with emphasis on some of the most novel approaches utilized to manufacture these structures, is also presented. **Section 3** reviews some of the most promising applications of density-graded structures with a focus on their load-bearing characteristics. Recent developments in the use of density-graded cellular solids in biomedical and acoustic applications are briefly discussed. Finally, **Section 4** presents a brief discussion on the recent efforts in the structural and property optimization of graded cellular solids. The latter has been a trending topic of research in recent years due to the advancements in computational algorithms and the advents in manufacturing of parts with complex geometries.

2. Density-Graded Cellular Solids

2.1. Graded Foams: Concepts and Fabrication

Foams are widely used as energy-absorbing components in various engineering applications. These structures can withstand large deformations at nominally constant stress levels, also referred to as plateau stresses.^[1] Load-bearing and energy absorption capacities of foams can be tailored by varying the microstructure and architecture of their cells.^[9] The macroscopic properties of foams are highly dependent on their nominal density. Lower-density foams generally possess lower stiffness, lower plateau stresses, and higher densification strains for a given base material. In contrast, the energy absorption behavior of foams

does not necessarily follow a particular trend in response to changing the nominal density; rather, it is discussed in terms of energy absorption diagrams via analysis of the experimental stress–strain behaviors of foams with different densities.^[10] In other words, the energy absorption metrics are often described in terms of the area below the stress–strain curve, thus depending on both strength and deformability. Spatial variation of the density in a foam structure using laminated layers with different nominal densities leads to the development of density-graded foams. One of the most important purposes of fabricating the so-called density-graded foam structures is to attain higher energy absorption capacities, while maintaining high strength at minimal structural weights.

Density-graded foams can be produced in several ways. In an early attempt by Gupta,^[11] graded syntactic foams were fabricated using an epoxy resin matrix that embedded glass microballoons with spatially variable volume fractions. Following this method, several fabrication processes have been invented based on the use of epoxy-microballoon slurries. Graded syntactic foams have also been produced with variable microsphere shell thicknesses.^[12] Graded syntactic foams produced in these works were capable of withstanding compressive strains significantly higher than the failure strain of their ungraded counterparts. It has also been shown that the arrangement of layers in particular ways can result in improved energy absorption and compressive strength in graded syntactic foams.^[13] To further improve the performance of syntactic foams, glass microballoons have been substituted by alumina and silica cenospheres.^[14–16] Doddamani et al.^[17] developed a novel approach to fabricate functionally graded syntactic foams with fly ash cenospheres.

In addition to syntactic foams, single-material density-graded foams have also been developed by Cusson et al.^[18] by applying a controlled thermal gradient on the foam compression molding system. Density-graded polyethylene foams produced in this way were shown to possess improved flexural moduli and impact stress mitigating properties compared with their uniform density counterparts. **Figure 2a–d** shows the schematic and micrographs of different syntactic-graded foams fabricated from glass microballoons and cenospheres and density-graded polyethylene foams processed by spatially modulated thermal gradients in the compression molding system. The ability to produce graded structures with seamless interfaces has been reported as one of the major advantages in producing these foam structures.

Due to their lightweight and high energy-absorbing capacities, graded metal foams have attracted tremendous attention recently.^[19,20] He et al.^[21] used a modified casting method to produce closed-cell graded aluminum foams. Compared with uniform density foams, graded samples exhibited lower peak stress and an extended plateau region. Hangai et al.^[22] fabricated similar metallic foams using the friction stir-processing method. Metal foams were synthesized with two porosity layers using different amounts of foaming agents. The same research group made a combination of open-cell aluminum foams, consisting of Al/NaCl composites through a sintering dissolution technique.^[23] Using powder metallurgy, Hassani et al.^[24] applied particle size variation along the longitudinal axis and fabricated functionally graded open-cell Al foams (see **Figure 2e–f**), where spherical granulated carbamide particles were used as space holders.

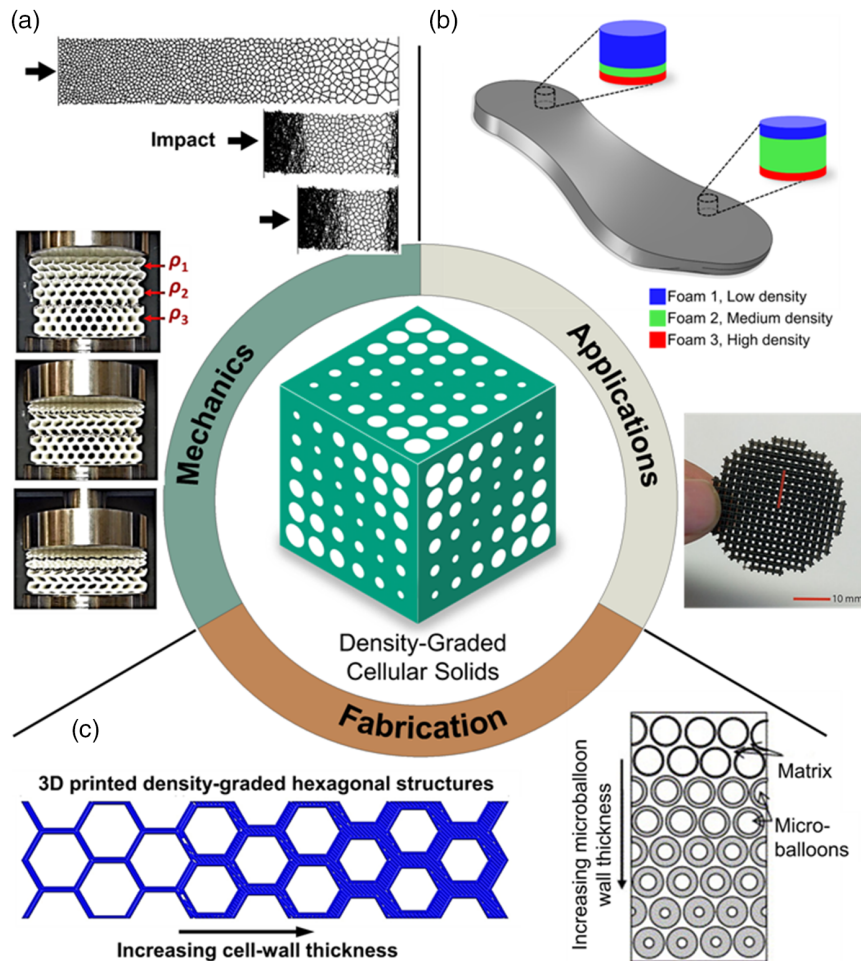


Figure 1. Mechanics, fabrication, and applications of density-graded structures are at the core of this review. a) Modeling and experimental characterization of the deformation response in density-graded foams (top)^[51] and lattice structures (bottom),^[104] b) examples of density-graded structures in biomechanics (e.g., design of shoe soles with enhanced cushioning properties^[218]), and acoustic applications (bottom),^[136] and c) fabrication of density-graded honeycombs by 3D printing (left)^[104] and graded syntactic foams (right).^[11] Panel a (bottom) reproduced from CC-BY open access Elsevier publication, 2019.^[104] Parts a (top) reproduced with permission.^[51] 2016, Elsevier. Panel b (top) reproduced with permission.^[218] 2020, Elsevier. Panel b (bottom) reproduced with permission.^[136] Springer Nature, 2018. Panel c left reproduced from CC-BY open access Elsevier publication, 2019.^[104] Panel c right reproduced with permission.^[11] 2007, Elsevier.

Metal-matrix syntactic-graded foams have also been produced in several previous studies. Similar to the concept of polymer-based syntactic foams, metal-matrix syntactic foams can also be processed by incorporating filler particles in a metallic matrix.^[25] In metal-matrix syntactic foams, the filler phase can be either hollow shells or porous particles.^[26,27] Two primary methods have been developed to produce functionally and density-graded metal-matrix syntactic foams: 1) variation of the volume fraction and size distribution of the hollow particles along specific directions throughout the structure and 2) use of multiple types of particles for tailored distributions of gradient properties. By controlling the distribution of microspheres during the centrifugal casting process, Ferreira et al.^[28] developed Al-matrix syntactic foams with spatially variable structures and properties. In another similar attempt, aluminum syntactic foams were developed through the random distribution of two different filler particles, that is, hollow ceramic and hollow iron.^[29] Movahedi et al.^[30] recently fabricated functionally graded syntactic metal foams using

two different filler particles (activated carbon and expanded perlite). A systematic comparison of the mechanical properties of these foams with conventional metallic foams revealed the superior energy absorption behavior of the graded structures. Movahedi et al.^[30] also demonstrated that the apparent yield stress, densification strain, and energy absorption responses of the examined graded structures were highly dependent on the constituents' density. Although not fully explored, the data in Movahedi et al.^[30] point to the possibility of achieving optimal mechanical properties through spatial modulation of the phases' densities in metal-matrix foams.

2.2. Characterization of the Mechanical Response of Graded Foams

In addition to the efforts dedicated to the processing and fabrication of graded foams, there have also been a plethora of

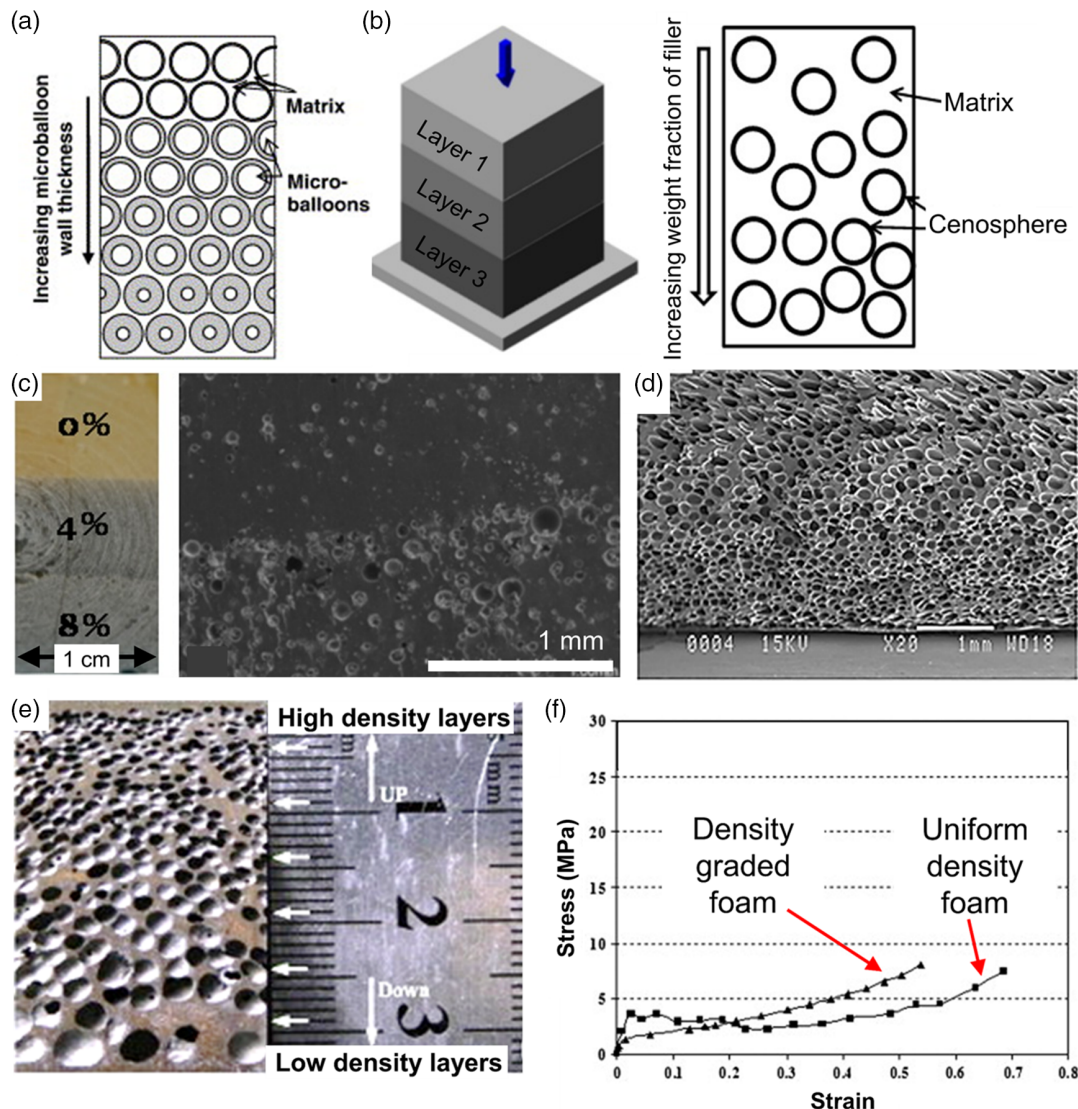


Figure 2. Density-graded polymeric foams. a) Schematic representation of functionally graded syntactic foams fabricated using glass microballoons as the filler.^[11] b) Schematic of the three-layered density-graded syntactic foams fabricated by embedding cenospheres in an epoxy matrix.^[17] c) Optical and scanning electron microscope (SEM) micrographs of density-graded syntactic foams showing the seamless interface between adjacent layers and a clear difference in the cenosphere concentration across the interface.^[17] d) SEM micrograph of density-graded polyethylene showing a continuous variation of cell size along the gradient (vertical) direction.^[18] Density-graded metal foams: e) optical micrograph of a cell-size-graded Al matrix foam produced by powder-space holder technique using spherical granulated carbamide as space holders. f) A comparison between the compressive stress–strain responses of density-graded and uniform density Al matrix foams indicating higher mechanical strength (at compressive strains > 0.2) and higher strain hardening response achieved through density gradation.^[24] Panel a reproduced with permission.^[11] 2007, Elsevier. Panel b reproduced with permission.^[17] 2012, Elsevier. Panel c reproduced with permission.^[17] 2015, Wiley. Panel d reproduced with permission.^[18] 2019, Sage. Panels e & f reproduced with permission.^[24] 2012, Elsevier.

research works focused on characterizing the mechanical response of these structures. Many of the studies in this area focus on the modeling and theoretical analyses of density-graded foams in response to external mechanical loads. For example, Chen et al.^[31] have used the Voronoi model to analyze the mechanical and energy absorption behaviors of closed-cell foams with spatially distributed porosities. Dynamic mechanical response of density-graded structures subjected to impact loading was investigated by Liang et al.,^[32] Yang et al.,^[33] and Zhou et al.^[34] In addition to simple geometries, functional and density-graded systems, including sandwich structures and metallic

tubes, were also analyzed in several numerical and analytical studies.^[35–37]

Experimental studies have been conducted to understand the constitutive mechanical response of density-graded foams subjected to quasistatic and dynamic loading conditions. Experimental studies conducted recently via in situ digital image correlation (DIC) measurements suggest that the main difference between the stress–strain response of uniform and density-graded foams lies in the fact that graded structures show a step-wise hardening behavior that occurs due to the sequential collapse of various density layers in the structure. Such a

sequential collapse mechanism starts with the weakest (lowest-density) region and continues throughout the higher-density layers. This step-wise collapse pattern is shown in **Figure 3a–c** for graded foam structures with continuous and step-wise gradients subjected to quasistatic loading.^[38,39] It is established that the sequential hardening takes place in graded foams regardless of the number and distribution of density layers present in the structure. Nevertheless, graded foams with distinct density layers show a more obvious step-wise hardening response in their global stress–strain response, as shown in **Figure 3b**.

In addition to quasistatic compression,^[21,40,41] drop weight impact^[42] and projectile impact tests^[43] are used to study the slow rate and low-velocity impact response of density-graded foams and characterize the high-energy and high-velocity impact response and crashworthiness of these structures. For example, Xia et al.^[44] conducted blast tests to analyze the effectiveness of density-graded foams for blast mitigation. Shock loading response of density-graded foams has been an active topic of research in several other investigations. Liu et al.^[45] used the shock wave theory to analyze the dynamic behavior of density-graded cellular rods subjected to axial impact. Similar theoretical studies were conducted by Shen et al.,^[46,47] wherein the compaction wave propagation patterns in density-graded foams were also analyzed using shock wave theory. Results obtained from these studies as well as those of Karagioza and Alves,^[48] Liu et al.,^[49] Wang et al.,^[50] Zheng et al.,^[51] and Chang et al.^[52] suggest that the shock wave propagation patterns in density-graded foams are highly sensitive to density distribution, also referred to as the gradient. It has been shown that the shock wave response in density-graded foams with a negative gradient (i.e., the higher-density layers are positioned toward the impact side), a double shock wave propagation mode, can develop. Such double shock wave phenomena take place when a forward compaction wave (formed at the impact end) and a backward compaction wave (formed at the distal end) propagate in opposite directions (see **Figure 3d**). The development of such double shock wave patterns alters the overall stress–strain and the energy absorption capacity of the structure, as the stress of the distal end can be more effectively mitigated in earlier deformation times. In contrast, density-graded foams with a positive gradient, that is, structures whose impact end is fabricated from lower-density components, deform with a single shock wave mechanism. In these structures, the shock wave propagation is more stable, and the overall energy absorption performance of the structure is improved. Observations and quantitative measurements of compaction waves and the verification of single versus double shock propagation modes (see **Figure 3d,e**) have recently been conducted in a series of studies that use ultrahigh-speed DIC.^[39,53–55] Full-field deformation measurements facilitated by DIC have been used to determine the acceleration fields and their corresponding inertia stress fields as metrics for tracking the propagation of compaction waves in uniform and density-graded foams.

The mechanical and shock propagation response in density-graded structures with more complex gradients and those subjected to complex loading conditions have also been characterized. These studies include nonlinearly varying continuously graded structures,^[49] structures with variable cross sections,^[56] and middle-high and middle-low density-graded foams.^[51] Chen et al.^[57,58] studied the dynamic behavior of graded foams

using the fluid structure interaction method, wherein the foam samples were subject to underwater blast loading. High-temperature dynamic response of graded cellular structures was investigated by Liu et al.,^[59] analyzing the influence of the thermal environment on the impact energy mitigation response of density-graded foams using finite-element simulations. It was found that the general shock propagation patterns (i.e., single shock and double shock wave propagation modes) persist in density-graded foams under thermal loading conditions. However, the presence of a temperature gradient along the sample axis can enlarge the deformed regions both for negative and for positive gradient cases. While a positive gradient function can lead to an enhanced impact energy absorption performance, the general impact mitigating efficacy of a graded foam is deteriorated as the thermal gradients intensify.

Graded foams have received particular attention in sandwich structures due to their enhanced energy absorption at low structural weights. The density gradation in sandwich panels can increase the critical velocity and kinetic energy required to induce failure, thus improving the panel's overall energy absorption capability.^[60] Using drop weight impact, Zhou et al.^[61] conducted an experimental study on graded-foam sandwich structures and highlighted the improved perforation resistance of these structures compared with uniform density foam cores. Zhang et al.^[62] studied the dynamic response of graded foams using ball impact tests and concluded that the placement of high-density layers in the proximal end improves the overall crashworthiness of a graded structure. In another work, Pollien et al.^[63] conducted bending tests on graded foam sandwich structures. While the mechanical performance of graded foams was shown to outperform that of single-density structures, the scope of using a lightweight graded structure was reported to be limited and impractical from a manufacturing perspective. Wang et al.^[64] studied sandwich composite panels with graded cores under shock wave loading. It was shown that in cases where lower-density foam layers were oriented toward the shock load, the structure was able to absorb the kinetic energy of the shock more effectively by undergoing large local compressions. These large compressive deformations reduced the amount of damage imparted to the structure. Besides experimental studies, numerous numerical studies address the dynamic and impact behavior of graded foam sandwich structures,^[65,66] clearly demonstrating that the impact mitigation performance of sandwich structures can be significantly enhanced when the core is made of a density-graded foam.

2.3. Graded Lattice Structures: Concepts and Mechanical Deformation Response

2.3.1. Definitions, Types, and Mechanical Characterization

Lattice structures are topologically ordered, 2D or 3D open-cell structures, consisting of one or more repeating unit cells with no gaps between cells.^[67–69] A lattice structure is an example of a cellular solid, although the terms are often used interchangeably.^[70] Natural cellular materials (e.g., wood, bone, cork, coral, bamboo, etc.) have been used for centuries, and their cellular structures have been replicated in modern times in the form

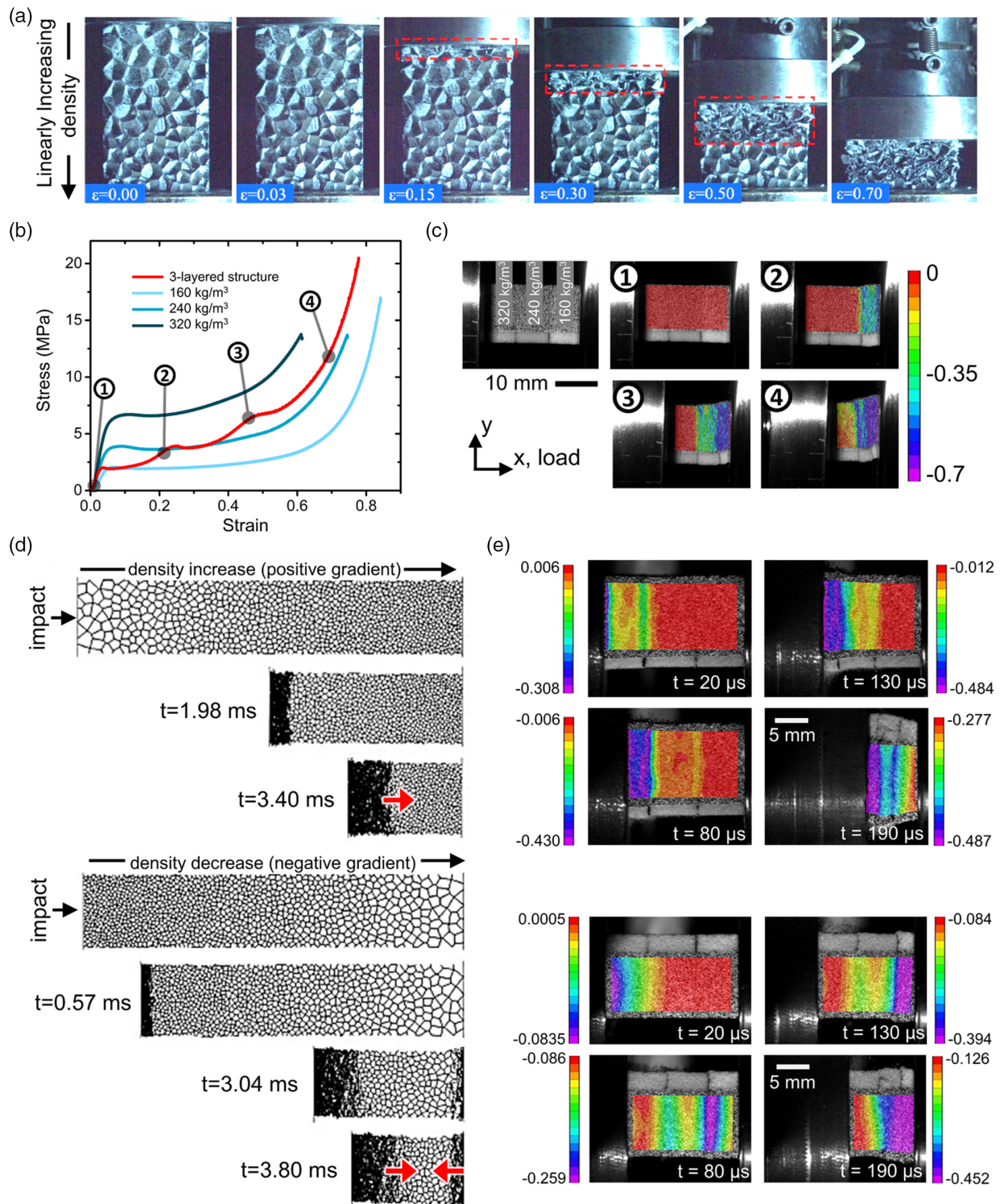


Figure 3. Layer-by-layer collapse mechanism in density-graded foams under quasistatic loading revealed by a) in situ imaging of density-graded foams with continuous gradation^[38] and b,c) DIC characterizations of discretely layered polyurethane foams.^[39] Numbers in (c) mark the corresponding stress/strain values in (b). Contour maps in (c) show the distribution of axial strain, ϵ_{xx} , in the layered structure. d) Modeling the crushing response of density-graded foams under impact loading conditions showing the development of single shock (top) and double shock (bottom) wave patterns.^[51] Similar experimental results are obtained by conducting impact tests on three-layered density-graded polyurethane foams with different gradients: e) impact load applied at the low-density side (top); impact load applied at the high-density side (bottom).^[39] The contour maps in (e) show the distribution of axial strain at various time instances after the impact. Panel a reproduced with permission.^[38] 2020, Elsevier. Panels b, c and e reproduced with permission.^[39] 2021, Elsevier. Panel d reproduced with permission.^[51] 2016, Elsevier.

of lattice structures and synthetic foams.^[71] Lattice structures are highly attractive for various applications, for example, biomedical,^[72] automotive,^[73] aeronautical,^[74] and energy absorption,^[75,76] to name a few, due to their favorable properties such as a low stiffness-to-weight ratio, tunable thermal conductivity, and impact resistance, all of which are the result of their highly porous structure.^[77]

Thermomechanical properties of lattice structures strongly depend on the architecture of their building blocks, referred to as “unit cells.” Lattice unit cells can be categorized as stretch dominated (stiff and strong) or bending dominated (flexible), depending on the mechanical response of the parent solid, nodal connectivity (i.e., number of struts joining a node), and cell topology. The latter can further be grouped into strut based and surface based.^[78,79] Strut-based lattice structures consist of a network of often prismatic struts connected at nodes. The number of struts connected at a given node dominates the lattice structure behavior under compressive loading conditions.^[80] Depending on the number of struts, S , and nodes, N , strut-based structures can be characterized by their Maxwell number, M , expressed as^[81]

$$M = S - 3N + 6 \quad (1)$$

Bending-dominated structures are those with a negative Maxwell number ($M < 0$). This condition implies that the number of struts should be smaller than that of stretch-dominated counterparts. Among all the strut-based unit cell lattice structures, the most widely used ones are body-centered cubic, face-centered cubic, and honeycomb structures. Other common unit cell types include diamond, cube, tetrahedral, and dodecahedron.

Besides strut-based unit cells, triply periodic minimal surfaces (TPMS) are the most common type of surface-based unit cells made of surfaces with mathematically defined structures repeated in three dimensions with a mean curvature of zero at every point.^[80] TPMS structures have been observed to possess highly repeatable additive manufacturability and uniform stress distribution, which stem from their unique geometric characteristics.^[81] Examples of TPMS are gyroid, Schwarz-diamond, and Schwarz-primitive structures (see **Figure 4a**). Gyroid pattern unit cells, naturally found in the microstructure of butterfly wings and adapted to become gyroid lattice structures, are the most extensively researched TPMS unit cells.^[82]

The compressive mechanical performance and energy absorption capacity of TPMS structures with and without density gradients have been investigated in numerous studies. For instance, quasistatic compressive behaviors of four different TPMS lattice structures were analyzed experimentally and numerically by Shi et al.^[83] While gyroid, diamond, and I-wrapped (IW) structures have a bending-torsional coupling deformation mode due to their relative density, gyroid and IW structures showed improved compressive mechanical performance but lowered energy absorption capacities. Yu et al.^[84] investigated the mechanical properties and energy absorption capacity of uniform and density-graded Schwarz-primitive and gyroid lattice structures (**Figure 4b**). While the Schwarz-primitive structures cracked in a layer-by-layer pattern and showed pronounced peak stress, the gyroid structures showed inconspicuous cracks. Al-Ketan

et al.^[85] investigated the effect of density gradation, cell-type grading, and lattice-type gradation in gyroid and diamond TPMS unit cells (**Figure 4c**). When tested perpendicular to the gradient direction, the density-graded structures exhibited shear band formation. The dominant deformation patterns were changed to a layer-by-layer compression and sequential collapse mode when tested parallel to the gradient direction. Han et al.^[86] analyzed the compressive mechanical properties of uniform and continuously graded porous scaffolds with Schwarz-diamond unit cells. Layer-by-layer deformation followed by step-wise densification mechanisms was also observed in the graded samples in the results of Han et al.^[86] The step-wise yielding and densification in graded structures were also observed by Liu et al.^[87] for density-graded TPMS gyroid and diamond unit cell lattice structures made from Ti–6Al–4V alloy. The deformation mechanism was observed to be dominated by shear deformation for structures with unit cell grading. The effect of different gradient patterns was studied by Afshar et al.^[88] using stretch-dominated (I-WP and primitive) and bending-dominated (diamond) polymeric TPMS structures. They observed that the deformation mechanism exhibited by the structures was informed by the gradient patterns. Higher deformability and lower failure strains were observed for structures graded longitudinally.

As another class of ordered cellular solids, mechanical metamaterials are artificially designed with micro/nanoarchitectures that derive their properties from their internal microstructure and geometry. By carefully engineering the unit cells in these metamaterials, unusual properties that do not rely on their chemical composition can be achieved. Metamaterials exhibit a wide set of mechanical and physical properties which are otherwise not found in nature. The expanded material properties have given rise to new potentials for various applications, where their unique properties can be exploited.

In recent years, the concept of auxetic metamaterials has invigorated tremendous research and technological interest. Auxetic metamaterials are structures that possess a negative Poisson's ratio. The negative Poisson's ratio implies that when an auxetic metamaterial undergoes uniaxial tensile deformation, it stretches in one direction, while expanding in the perpendicular direction. Under compressive forces, auxetic structures contract in the axial and transverse directions.^[4] The artificial hardening behavior in auxetic structures, which is attributed to the negative Poisson effect, enables them to have higher load-bearing capacities than conventional cellular structures. Furthermore, auxetic metamaterials have been shown to exhibit higher fracture toughness, shear modulus, strength-to-weight ratio, resistance to fatigue crack propagation, and enhanced vibration damping properties.^[4,6] The combination of these favorable attributes has led to the widespread use of auxetic structures as one of the most viable candidates for impact resistance and energy absorption applications. Chiral, re-entrant, and double arrowhead are among the most widely used cell geometries exhibiting auxetic behavior.

The in-plane dynamic behavior and energy absorption characteristics of uniform, graded auxetic antichiral, and hybrid chiral structures (see **Figure 4d**) have been analyzed by Qi et al.^[89] It was observed that the gradient effect impacts the graded hybrid chiral structures more significantly than the antichiral structures. Wu et al.^[90] studied a cell-wall angle graded auxetic structure for

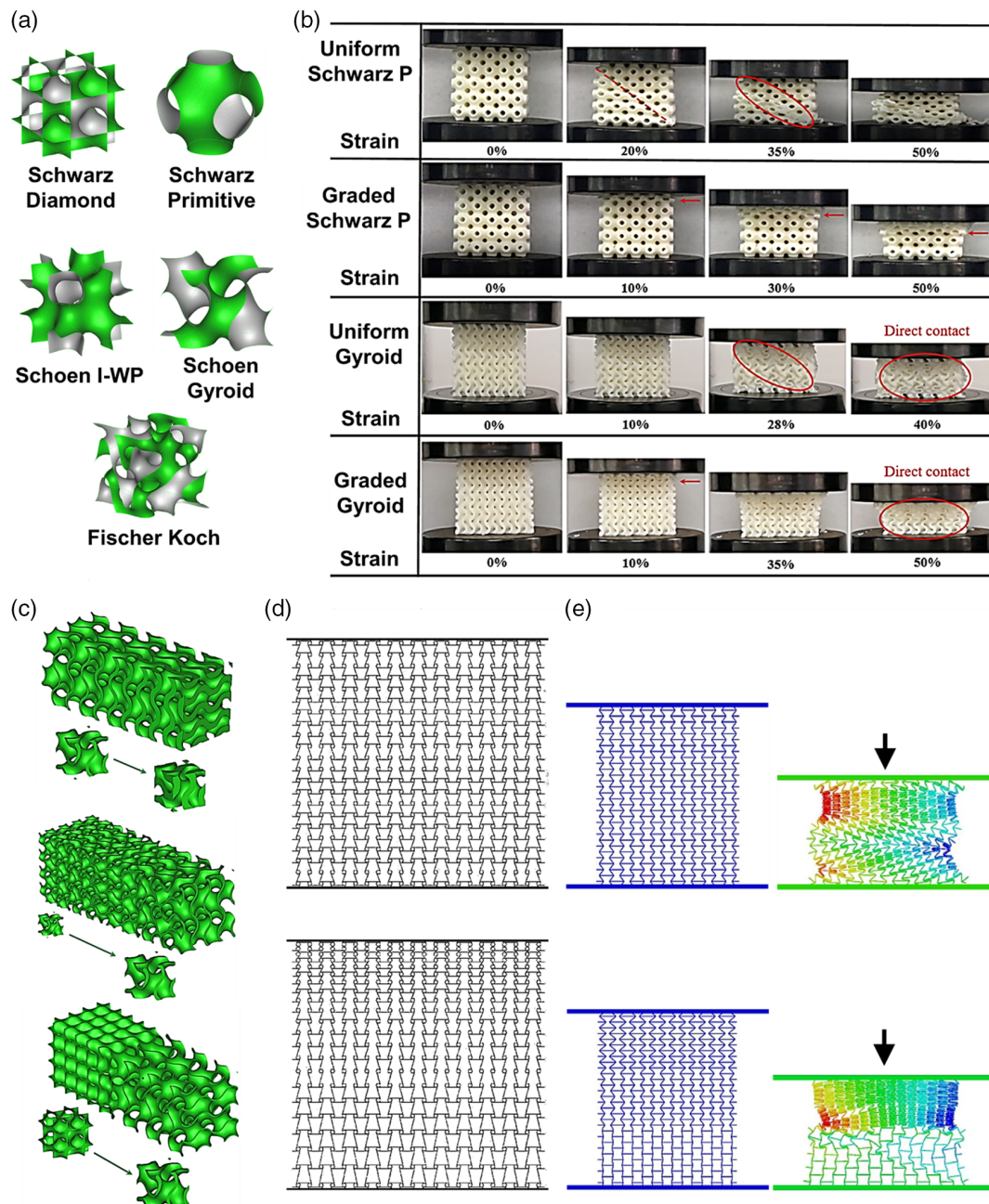


Figure 4. a) Examples of TPMS lattices.^[85] b) Deformation behavior of uniform and density-graded Schwarz P and gyroid structure under quasistatic compression.^[84] Uniform density structures show a shear band formation whereas the deformation of density-graded structures is exemplified in a sequential layer-by-layer collapse that initiates from the low-density layers and propagates through the higher-density areas. c) Various gradation approaches used in the production of graded TPMS structures: density gradation (top), unit cell size gradation (middle), and multimorphology lattice gradation (bottom).^[85] d) Schematic of uniform (top) and graded (bottom) hybrid chiral structures.^[89] e) An example of density gradation by cell wall angle variation in re-entrant structures. Ungraded (top) and layer-wise graded (bottom) structures show vastly different deformation patterns when subjected to compressive loads.^[90] Panels a & c reproduced with permission.^[85] 2020, Elsevier. Panel b reproduced with permission.^[84] 2019, Elsevier. Panel d reproduced with permission.^[89] 2019, Elsevier. Panel e reproduced with permission.^[90] 2020, Elsevier.

enhanced energy absorption applications. As shown in Figure 4e, under compression, uniform and graded structures show significant differences in deformation patterns. When subjected to quasistatic compressive loads, the energy absorption response improvement was significant due to the graded design.

However, improved strain energy absorption was only achieved when the crushing direction was along the weak-to-strong direction (i.e., a positive gradient function). Jin et al.^[91] showed that the graded auxetic structures used as sandwich panel cores can improve the resistance of panels to blast loading compared with

ungraded cores when the higher density side of the structure is positioned toward the impact side. Novak et al.^[92] reported that the plateau stress (progressive/regressive) in graded auxetic structures fabricated from Ti–6Al–4 V subjected to impact loading is dependent on the direction of the gradient. Interestingly, the latter two observations have been consistent with those made on density-graded foams and lattice structures, implying that a universal deformation mechanism may exist for different types of density-graded cellular solids irrespective of their cell type, architecture, and cellular order.

Design and development of gradient 2D auxetic metamaterials have been reported in some recent reports, as well.^[93,94] Spatially controlled morphology and structural shape changes, especially when subjected to large tensile deformations, make the new generation of these graded 2D structures promising for a number of different applications, including but not limited to soft robotics^[95] and protective structure.^[94]

Metamaterials inspired by origami (ancient Japanese art of folding paper) have also gained widespread attention in recent years. Miura-Ori is one of the most studied types of origami structures.^[96] 2D- (gradient along x -direction) and 3D (gradient along x - and z -directions)-graded origami structures based on the Miura-Ori pattern were studied under quasistatic compressive loading conditions by Yuan et al.^[97] It was observed that there was a sequence of buckling and collapse throughout the rows, which originated as a result of the innate self-locking graded geometry. Kirigami is another variation of origami that includes cutting the paper creases in conjunction with folding to create cellular tessellations.^[98] A kirigami sandwich structure made of half-graded auxetic honeycomb and half re-entrant honeycomb was manufactured using woven Kevlar prepreg for compression and edgewise loading.^[99] Due to the negative Poisson's ratio, the mechanical behavior of the structure was reported to be dependent on loading direction. Different failure mechanisms were observed with the graded sandwich panels under quasistatic edgewise loading.

2.3.2. In-Plane Versus Out-of-Plane Mechanical Response of Density-Graded Lattice Structures

A number of theoretical and experimental works were conducted on the in-plane and out-of-plane mechanical properties of density-graded lattice structures under static and dynamic loading conditions.^[100] Density-graded lattice structures have been thoroughly researched and reported to exhibit a layer-by-layer deformation behavior when subjected to compressive loads.^[101,102] The layer-wise deformation patterns in these structures stem from the deformation and collapse of the lower-density layers before higher-density sections. This behavior often leads to an apparent step-wise stress–strain curve that has been reported in honeycombs made from various materials and lattice types.^[103–105] It is worth mentioning that the number of steps observed in the stress–strain curves of density-graded structures corresponds with the number of density layers present in the structure (see **Figure 5a–c**). The step-wise response is exemplified in both in-plane and out-of-plane deformation conditions, except in graded structures, like in uniform density lattices, out-of-plane loading is generally associated with higher

strengths. The step-wise behavior is due to the different micro-scale deformation responses in out-of-plane (cell-wall and strut buckling) versus in-plane (cell-wall bending) loading.^[1,106]

The mechanical behavior of density-graded gyroid cellular structures with continuous gradients under in-plane compression was characterized by Yang et al.^[107] It was observed that while samples graded perpendicular to the loading direction exhibited deformation behaviors similar to uniform density structures, samples with gradients parallel to the loading direction showed a layer-by-layer collapse with extended plateau regions, higher Young's moduli, and improved energy absorption. Tao et al.^[108] studied the out-of-plane crushing strength and energy absorption of graded honeycomb structures using numerical simulation, relating the in-plane gradient to improved crushing strength and specific energy absorption of the honeycomb structures by about 70%. Also, severe plastic deformation mainly concentrated at the intersecting cell walls, leading to a larger portion of the strain energy dissipated in that area. Similar studies were conducted by Kumar et al.,^[109] wherein the mechanical strength and energy absorption response of honeycomb structures under out-of-plane loads were investigated. It was reported that a geometrically tailored design made possible by varying the cell-wall thickness along the out-of-plane direction can lead to significant changes in the energy absorption characteristics of the structure.

The ability to modulate the energy absorption capacity of hexagonal honeycombs with in-plane gradients has been proven promising, especially in low-velocity impact loading scenarios (see **Figure 5d–f**). The improved strain energy absorption capacity in density-graded honeycombs has been reported for structures fabricated from both elastoplastic^[103] and hyperplastic materials.^[104] Recent trends in the applications of flexible honeycombs with in-plane gradients have the potentials to open new doors to the design of nonpneumatic tires and wheels (**Figure 5g**) with superior performance (reduced noise, increased durability, multiple impact sustainability, and less heat build-up) at lower weights compared with their conventional counterparts.

2.4. Fabrication of Graded Lattice Structures

Conventional methods of design and fabrication of engineering materials are often not applicable to density-graded lattice structures as they contain delicate unit cells. Following the advent of additive manufacturing technologies in conjunction with the advancements in computer-aided design software development, optimal design and fabrication of complex lattice structures with density/functionality gradations have become possible. This section discusses the most common fabrication methods used for the processing and fabrication of density-graded lattice structures.

2.4.1. Stereolithography (SLA)

Considered the first rapid prototyping manufacturing method, stereolithography (SLA) is a photopolymerization procedure used in several engineering areas. A laser beam is directed toward a point on the photosensitive resin surface to trigger the polymerization process. The laser beam then moves to a different spot and rasters until a layer is cured. The fully cured layer is then lifted,

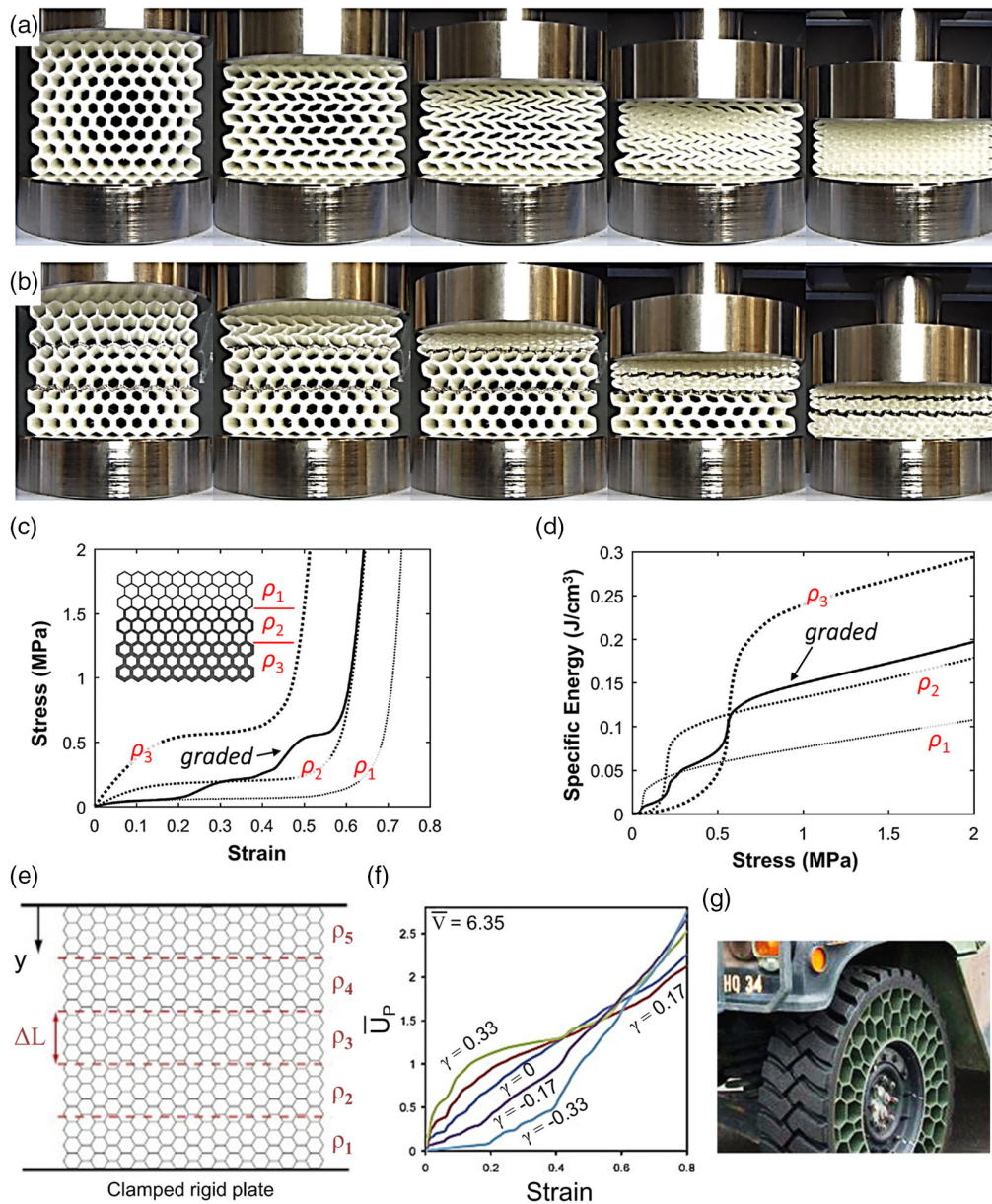


Figure 5. In-plane deformation behavior of a) uniform density and b) three-stage graded hexagonal honeycomb structures fabricated from TPU. c) Stress–strain and d) energy absorption responses of the three-stage flexible honeycombs. Dotted curves represent the behavior of uniform density structures. The number of stress plateaus in graded structures corresponds with the number of density layers present in the structure.^[104] e) Schematic and f) normalized plastic strain energy dissipation of elastoplastic honeycombs with various gradients under impact.^[103] Density gradient is denoted by the parameter, γ , defined as: $\gamma = (\rho_{i+1} - \rho_i)/\Delta L$. g) A nonpneumatic tire with flexible honeycomb spokes (Source: <https://www.compositesworld.com/articles/tires-that-never-go-flat>). Panels a–d reproduced from CC-BY open access.^[104] 2019, Elsevier. Panels e & f reproduced with permission.^[103] 2011, Elsevier.

and a new layer is formed based on the geometric details in the G-code file. Gonzalez et al.^[110] used this process to fabricate a 3D hemimaxillary bone-like structure using aluminum oxide and polymeric mixtures with the aid of ceramic SLA printing equipment. They observed that the structure could be sintered defect free, and the process is appropriately scalable for wall thicknesses smaller than 100 μm . Liu et al.^[111] also investigated the compressive mechanical behavior of topology-optimized graded

structures made by SLA and discovered that their mechanical behavior is dependent on the type and arrangement of the unit cells.

2.4.2. Material Extrusion

Developed in the 1990s, material extrusion, commonly referred to as fused deposition modeling (FDM) trademarked by

Stratasys, is one of the fastest-growing additive manufacturing methods for fabricating thermoplastic materials.^[112] Material extrusion, also known as fused filament fabrication (FFF), produces 3D objects by a molten thermoplastic deposited into successive 2D layers.^[113,114] The process entails the extrusion of a molten filament through a nozzle, building up a 3D object layer by layer, and thus is regarded as a bottom-up method of manufacturing. This process is popular due to its ease of application and its ability to fabricate complex geometries at low costs. One of the major benefits of this additive manufacturing technique is attributed to the simultaneous feeding of the filament and layer-by-layer printing of the object. Therefore, it is possible to adjust the type and quantity of the deposition both temporally and spatially. This feature makes the material extrusion process a practical method of fabricating graded and multimaterial structures.

Bates et al.^[104] fabricated density-graded honeycomb structures using thermoplastic polyurethane (TPU) by the FDM method. The architected structures were graded discretely (two, three, and five different densities in nine layers) and continuously (nine different densities). Through a series of experimental characterizations, they observed that the density gradation could modify the mechanical damping of the structure. There was also an increase in the energy absorption capability of the honeycomb structures. The experimental data obtained by Bates et al.^[104] were used as the input to a modeling effort, in which the superior load bearing and strain energy absorption performance of 3D-printed TPU honeycombs were analyzed and optimized.^[115] Material extrusion was also used to fabricate four graded cellular structures with different unit cell shapes (cylindrical, square, hexagon, and triangular) by Duraibabu et al.^[116] The energy absorption capability of all four samples was investigated as a function of their pore size, shape, and relative density. Duraibabu et al.^[116] found that graded hexagonal honeycomb structures have the highest energy absorption capacities.

2.4.3. Directed Energy Deposition (DED) and Selective Laser Sintering/Melting (SLS/SLM)

Direct energy deposition (DED) technique involves introducing focused thermal energy, such as a laser, electron beam, or a plasma arc, to fuse coaxial material feedstock (metal powders or wire) by melting and quick solidification to form a sintered layer on a substrate.^[117,118] While the DED method has mostly been utilized as a coating process, it has also been proven suitable for fabricating density-graded structures. When using wires, graded 3D objects can be produced by controlling the feedstock speed. Metallic density-graded 3D objects can also be fabricated by adjusting the volume of metal powders fed into a melt pool under a moving laser.^[119]

Selective laser sintering (SLS)/selective laser melting (SLM) methods are categorized as light-assisted additive manufacturing methods. The main difference between DED and SLS/SLM methods is that in the latter, an entire area within a powder bed is melted/sintered, enabling the creation of a 3D object in a layer-by-layer pattern, while in the former, melting/sintering process is generally carried out in a point-by-point fashion.^[120,121]

SLM method has been utilized to manufacture and study the mechanical properties of density-graded (by varying strut diameter) structures against their uniform density counterparts by Maskery et al.^[122] While both graded and uniform density structures absorbed the same amount of energy before densification, the strain at which the graded structure densified was measured to be lower than that of the uniform structures. Choy et al.^[123] investigated the mechanical properties of density-graded cubic and honeycomb Ti–6Al–4V lattice structures fabricated by SLM. The strut diameters of the lattice structures were varied both discretely and continuously along the cell layers. It was observed that three out of the four fabricated density-graded samples absorbed more energy and attained higher plateau stress than the uniform density samples. Also, unlike the density-graded samples whose compressive mechanical deformation was exemplified by a sequential and layer-by-layer pattern (similar to those shown in Figure 4b), the uniform density samples showed abrupt shear failure with diagonal cracking across the whole structure.

3. Other Applications of Density-Graded Structures

3.1. Acoustic Applications

An essential application of density-graded structures lies in the field of acoustics. For example, the damping of acoustic energy is of great interest in numerous scenarios. Because of their lightweight and porous structures, cellular solids serve as promising candidates for noise control, especially in achieving sound absorption within a wide-frequency range with moderate space occupancy. These cellular structures and materials can absorb acoustic energy through dissipation and viscous losses inside them. For example, foam materials with high porosity have been widely used for noise mitigation.^[124] The acoustic properties of these foams are dependent on the pore size, porosity level, and mechanical properties of the base material.^[125] While foams with uniform pore sizes have been reported to exhibit effective sound absorption, by functionally designing the microstructures of the foams, including graded pore sizes, their acoustic properties can be further enhanced. Ke et al.^[126] reported an improved absorption coefficient of Al alloy foams with graded pore size manufactured by melt infiltration method. A graded bio-based foam structure is also proposed, and a 9% increase in average absorption is observed (Figure 6a).^[127] Following this concept, several layered or graded foam structures have been developed and optimized for noise control applications.^[128–132] Better absorption characteristics in bandwidth, absorption coefficient, or low-frequency performance are demonstrated. The behavior of composites with gradient impedance and density is also systematically studied, and it is shown that better low-frequency absorption can be achieved using a layered structure.^[133] The graded configuration of the mesoscale structures provides additional interactions between acoustic waves and structures, leading to better acoustic properties.

Besides the microstructural design of the cells in stochastic (nonordered) structures, the acoustic properties of periodic (ordered) structures (e.g., phononic crystals and

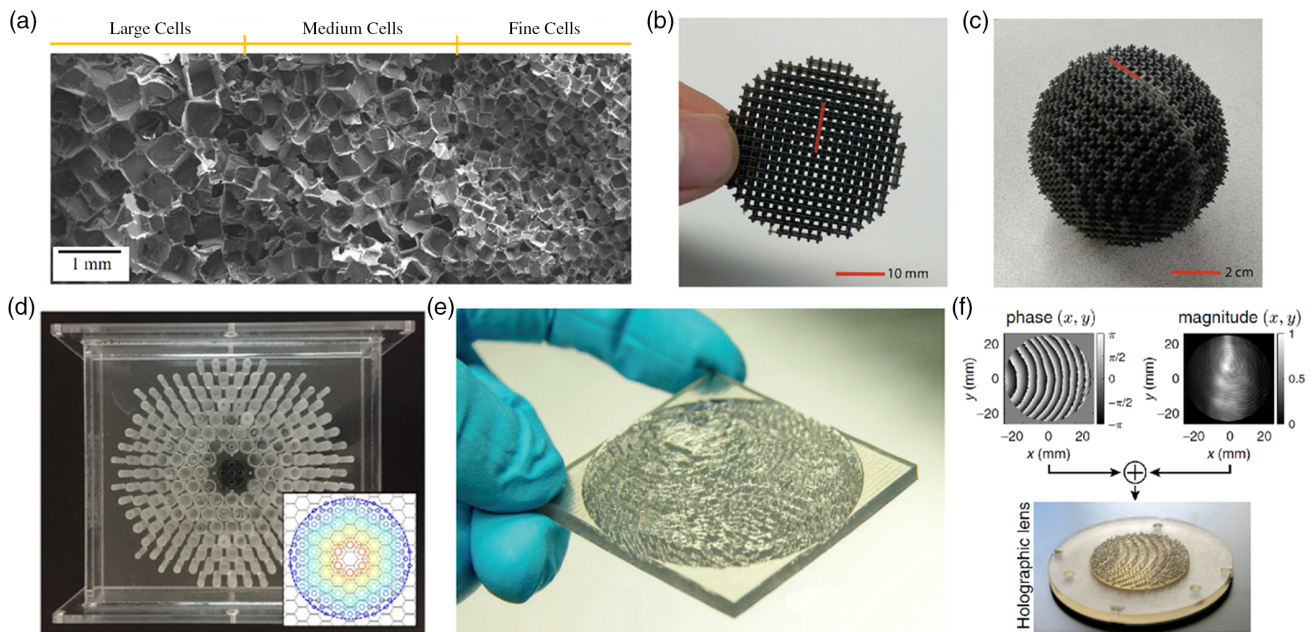


Figure 6. Density-graded structures for acoustic applications: a) Functionally graded foam structures for enhanced acoustic absorption.^[127] b,c) 2D and 3D Luneburg lenses for acoustic imaging. The refractive indices of the unit cells vary in the radial direction.^[136] d) Graded phononic crystal structures for acoustic focusing and energy harvesting.^[143] e) Schematic showing a holographic acoustic lens capable of delivering complex acoustic fields.^[159] f) Gradient-index lens used in biomedical ultrasound by forming desired pressure distribution inside the skull.^[174] Panel a reproduced with permission.^[127] 2015, Springer Nature. Panels b & c reproduced with permission.^[136] 2018, Springer Nature. Panel d reproduced with permission.^[143] 2020, American Institute of Physics (AIP). Panel e reproduced with permission.^[159] 2016, Springer Nature. Panel f reproduced with permission.^[174] 2019, American Physical Society (APS).

metamaterials^[134] are also investigated for wave control applications. By designing the unit cells hierarchy, the propagation of acoustic waves through the structure can be manipulated. For instance, lenses capable of tuning the propagation of acoustic waves can be obtained by stacking cellular structures with gradually varying indices. A prime example is the Luneburg and gradient-index lenses that can bend waves to a focal spot on the opposite surface of the lenses. Because of their minimal spherical aberration and wide field of view, these lenses have been widely used in acoustic focusing and imaging (Figure 6b–c).^[135,136] When integrated with a backing layer or an absorbing core, these lenses can also be used for retroreflection,^[137] sound absorption,^[138–141] or energy harvesting (Figure 6d)^[142,143] by routing acoustic waves to the target location. Graded metamaterials have also been used for impedance matching in ultrasonic transducers and other wave engineering devices.^[144–146]

In recent years, gradient-index or functionally graded metamaterials have been extended to planar versions, where graded scatterers are patterned in the lateral direction. These quasi 2D structures are called metasurfaces and have shown to exhibit unprecedented wave manipulation potentials.^[147] By controlling the local amplitude and phase of the transmitted or reflected acoustic waves, various functionalities have been proposed and realized, including wavefront modulation,^[148–153] asymmetric propagation,^[154–158] and acoustic holography (Figure 6e).^[159–162] Specifically, holographic lenses are also applied in fluid environments for the patterning of particles and cells.^[163–165] This enables label-free and high-throughput manipulation of bioparticles by controlling the acoustic pressure distribution and fluid motion. These metasurfaces can realize

different functionalities with minimal space requirement due to their thin thickness, which is often important in engineering applications. For example, Yang et al.^[166] developed an ultrathin broadband acoustic absorber using graded patterned resonators. The absorber is causally optimal as its thickness reaches the lower bound dictated by the law of causality. Other similar absorbing structures have been proposed by combining unit cells with gradient geometries.^[167–170] Compared with absorbers composed of uniform unit cells, introducing graded structures often results in a broader bandwidth, reduction of the thickness, or improved absorption coefficient. Such an improved functionality is a result of cell-to-cell coupling and synergic effects, which can be absent in uniformly structured materials. In addition to the aforementioned functionalities, graded acoustic metasurfaces have also found applications in advanced manufacturing,^[171] communication,^[172,173] and biomedical ultrasound (Figure 6f),^[174] to name a few.

3.2. Biomedical Applications

Bioinspired cellular structures have also attracted tremendous attention in biomedical applications. From artificial tissues to advanced implant design, the emergence of natural and biologically inspired structures has been evident in recent decades.^[175] Metamaterials that resemble the structure and performance of natural graded structures (such as bone, bamboo, etc.) have begun to find applications in biology and medicine. One important area that has highly benefited from the recent developments in architected and metamaterials is cell culturing in 3D environments. For instance, density-graded scaffolds that mimic the gradients

in native tissues have been synthesized by Nie et al.^[176] via a thermally induced phase-separation method. The novel continuous gradation method was shown to allow for precise adjustment and control of macropore sizes in the scaffold (see **Figure 7a**). 3D nanolattice scaffolds with applications in bone tissue growth were fabricated by Maggie et al.^[177]. The linear arrangement of tetrakaidecahedron unit cells with various strut sizes and different coatings was used by Maggie et al.^[177] to establish a stiffness gradient. In another scenario, auxetic scaffolds with a tunable Poisson's ratio were fabricated and demonstrated to be useful in cell differentiation applications.^[178] Because of their strain concentration effect, auxetic and honeycomb metamaterials have also been used in stretchable sensors and supercapacitors with enhanced sensitivity and capacity.^[179,180] In addition, studies have been conducted by leveraging the unconventional mechanical effects of metamaterials to achieve enhanced structural properties. For instance, metamaterial-inspired implants have been designed

to mitigate bone implant interface failure and improve the longevity of the implants (Figure 7b).^[181] In contrast, hierarchical and density-graded metamaterials provide better energy absorption and load-bearing functionalities geared toward biomaterials.^[182–184] Besides the intrinsic characteristics, another concept in developing biometamaterials is their interaction with external fields. Metamaterials can interact with electromagnetic, acoustic, or elastic waves to modulate the propagation of waves, enabling another layer of sensing and actuation in biomedical applications. For example, metamaterial-based microwave and terahertz sensors have been used in biomedical analyses.^[185,186] In ultrasound imaging applications, graded metamaterials are demonstrated to be useful for enhanced sensitivity^[187,188] and aberration correction.^[187,189] Because of the large potential of metamaterials and the importance of biology and medicine in the contemporary society, we anticipate that more work will be done to bring the technology into real-life products.

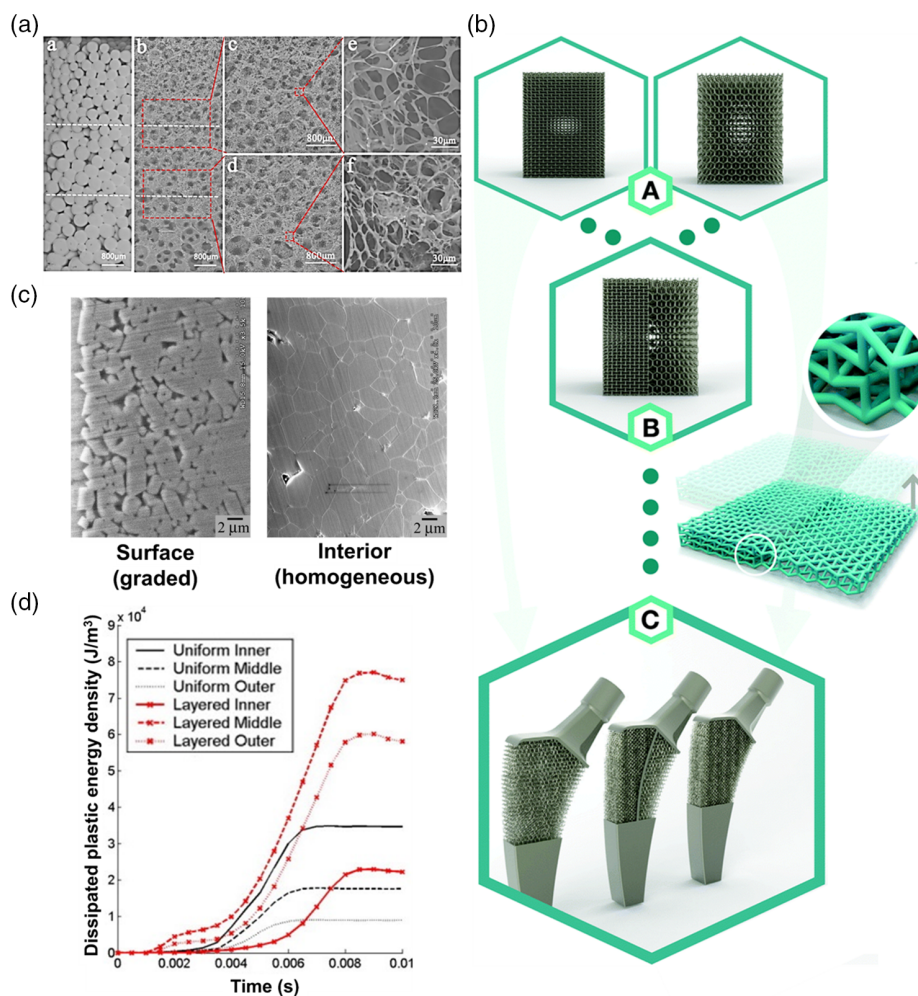


Figure 7. a) Continuous pore size gradient in a poly(L-lactic acid) scaffold produced by leaching sugar particles (shown in a).^[176] b) Schematic drawing of auxetic and conventional metamaterials, hybrid metamaterials, and meta implants shown in A, B, and C, respectively.^[181] c) SEM micrographs showing the near-surface (graded) and interior (homogeneous) morphologies of glass–alumina structures produced by sintering.^[194] d) Variation of dissipated plastic energy density with respect to time determined for uniform and three-layered density-graded equestrian helmet liners subjected to low energy impact.^[200] Improved performance of graded liners in dissipating the energy of the impact is evident. Panel a reproduced with permission.^[176] 2016, Elsevier. Panel b reproduced with permission.^[181] 2018, Royal Society of Chemistry. Panel c reproduced with permission.^[194] 2012, Elsevier. Panel d reproduced with permission.^[200] 2009, Elsevier.

In biomimicry, hierarchical formation is a critical feature that hinges on the continuous and spatial variation of structure/composition. Biomimetics adopts the basic concepts of material/structure gradation to promote and optimize several functionalities. For instance, the concept of porosity gradation is implemented for skeletal replacements to minimize stress shielding.^[190,191] Similar ideas have been implemented for dental implants to facilitate osseointegration.^[191] The functionality of dental implants changes at the jawbone boundary, inside and outside the jawbone.^[192] Due to the development of normal stresses around conventional single-metal implants, the possibility of losing bone density around the implant area, also known as stress shielding, can be increased. Graded implants are proven to be advantageous over conventional single-material implants in reducing stress shielding (Figure 7c)^[193–195] and preventing thermomechanical failure with improved biocompatibility.^[196] In addition, porous functionally graded implants have the potential to match Young's modulus of the bone, leading to the reduction of the residual bone removal process.^[197] The density/functionally gradation concepts also shed light on the aortic valve (AV) design. Under physiological conditions, graded AV leaflet is shown to experience large transmural stress variations.^[198] Osteoblasts' accumulation, bone formation, and vascular formation can be improved by controlling the spatial porosity (i.e., density modulation) in the structure.^[199]

In addition to the applications described earlier, the use of density-graded foams in biomechanics has also been documented. Design and development of highly energy-absorbing foam structures for helmets and footwear are among these applications. Graded foam liners with three density layers were shown to have the capability to reduce peak acceleration by expanding the contact area, better distributing the impact stress and consequently increasing the dissipation of plastic energy density in equestrian helmets (see Figure 7d).^[200,201] Shock absorption performance of shoe midsoles has been shown to improve substantially through density gradation.^[202]

4. Current and Future Efforts in Property Optimization of Graded Structures

While density-graded cellular structures have found applications in numerous areas, more remains to be done to further mature this field. Despite their usefulness in many aspects, structures and architectures of density-graded parts have to be judiciously designed and engineered so that they display desired properties, which is often a cumbersome task. The future of density-graded cellular structures calls for the design of these structures readily available for desired applications. As such, the rational design and optimization of these structures have become an important topic. Fueled by the recent developments in advanced optimization techniques, including machine learning, recent years have witnessed a growing interest in implementing these techniques to further push the boundaries of density-graded structures. These optimization tools (e.g., topology optimization,^[203–205] genetic algorithms,^[206] and machine learning^[207,208]) have been used at the microscopic- (i.e., the architecture of the cells) and the macroscopic-level^[209–211] (i.e., the mesoscale geometry and gradation of the cellular structures) designs in the search for lattice

and cellular geometries that lead to optimal mechanical properties at reduced structural weights. For example, using a gradient-based algorithm, Wang et al.^[212] determined the optimal truss lattice structure for arbitrary loadings in the low-volume limit. Berger et al.^[213] demonstrated extreme elastic properties through a data-driven design approach. Different from conventional design approaches, these optimization methodologies only require limited (or even zero) prior knowledge in the search for the optimal structures and exhibit great flexibility.

In addition to the data-driven optimization studies, there have also been recent efforts to develop optimized “application-specific” graded structures. For instance, Das et al.^[214] developed a multiphysics topology optimization technique to optimize a graded porous structure with an enhanced heat dissipation response by controlling the pore size and resolution. Cheng et al.^[210] proposed a stress constraint-based topology optimization model to minimize the total structure weight. Their model uses the asymptotic homogenization method to calculate the lattice structure's effective elastic properties in terms of design variables, whereas a multiscale failure model has been used to calculate yield strength. The proposed lattice structure was used for weight minimization purposes. A novel topology optimization technique was proposed to minimize the lattice structure's weight with a uniform variation of density by Li et al.,^[215] in which the variable-density gyroid structure was generated and optimized for superior load-bearing performance. Daynes et al.^[216] developed an optimization technique based on a novel biomimetic methodology to minimize the mechanical compliance of graded lattice core structures. In a recent effort by Panesar et al.,^[217] various topology optimization strategies were compared. It was concluded that although density gradation may not be the most efficient topology optimization strategy in terms of processing efforts, it can lead to high structural resilient designs. The significance of density-based topology optimization strategies that are especially applicable to additive manufacturing processes was studied in detail in a recent review by Plocher and Panesar.^[95]

Another optimization technique is the facile analytical optimization methodology, which has been proven effective in designing and developing density-graded foams and lattice structures for enhanced load-bearing and impact energy dissipation at reduced mass.^[40] The analytical gradient optimization methods have recently been utilized to develop density-graded flexible foams for footwear application^[218] and in density-graded honeycomb structures for structural applications.^[115] **Figure 8** shows examples of some recent efforts in the design and development of density-graded foams and lattice structures with optimal gradients.

As advanced manufacturing techniques have become an important means for the fabrication of graded structures, research effort has also been devoted in optimization with the consideration of manufacturing compatibility^[219–221] and novel material systems. Recent papers by Plocher and Panesar^[222,223] are examples of some of the most recent efforts, in which novel manufacturing methods are combined with high-performance materials to pursue of the design and property optimization of graded lattice structures. The advancement in computer clusters and numerical algorithms, in contrast, makes the optimization process more efficient and less expensive. Nevertheless, research efforts are still needed for the optimization of density-graded structures in a variety of applications.

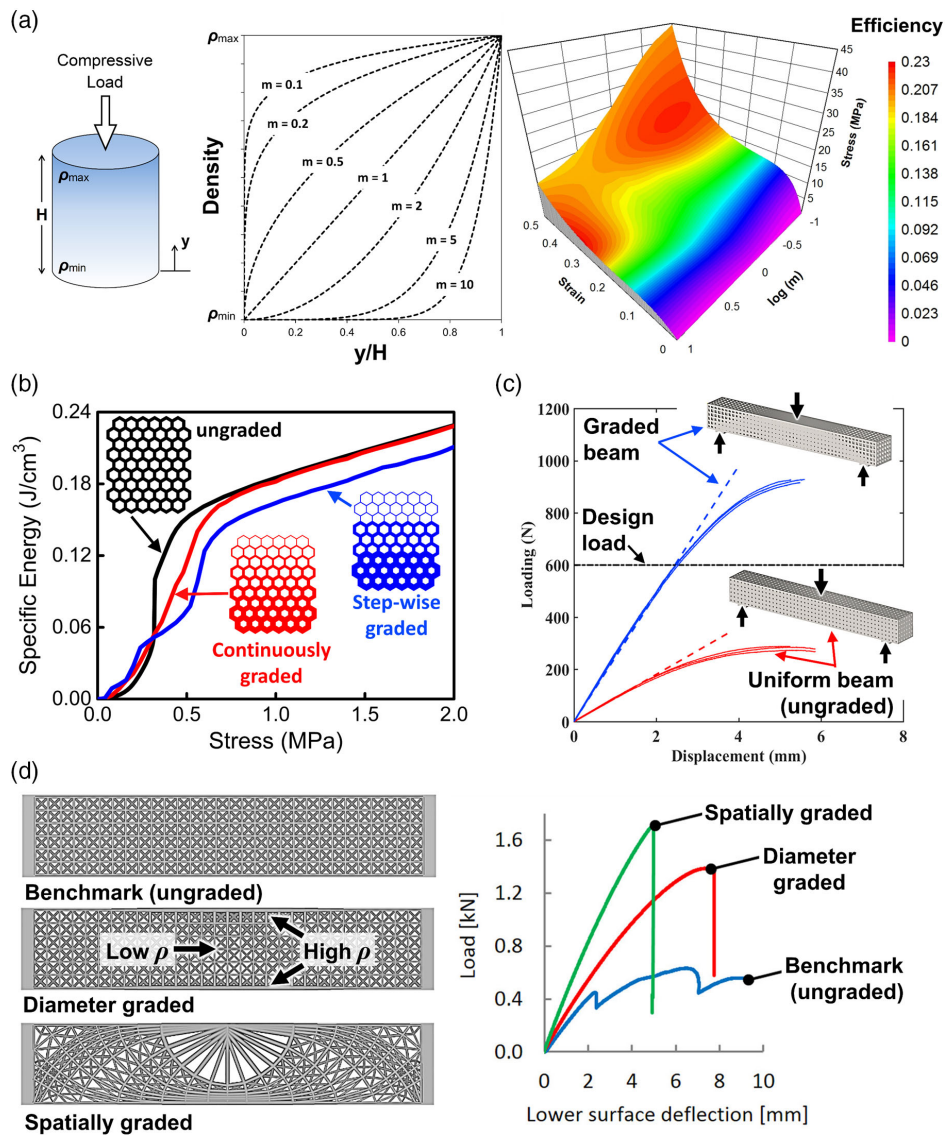


Figure 8. a) Optimization of density-graded polyurethane foams with various gradient functions controllable by the gradation exponent, m , in $\rho(y) = \rho_{\min} + [\rho_{\max} - \rho_{\min}](y/H)^m$. The generated efficiency (absorbed strain energy normalized by stress) maps shown on the right can be used to identify the optimal gradients.^[40] b) A comparison of ungraded, continuously graded, and step-wise graded hexagonal honeycombs used for the optimization of load bearing and energy absorption response in flexible honeycombs.^[115] c) A comparison between the flexural behaviors of uniform (ungraded) and density-graded beams with optimal spatially variable gradients.^[210] d) Ungraded, diameter-graded, and spatially graded (with optimal structure) beams with their corresponding load–deflection curves shown on the right. Both graded structures outperform the ungraded beam in terms of flexural stiffness and strength.^[216] Panel a reproduced with permission.^[40] 2016, Elsevier. Panel b reproduced from CC-BY open access.^[115] 2020, Elsevier. Panel c reproduced with permission.^[210] 2019, Elsevier. Panel d reproduced with permission.^[216] 2017, Elsevier.

Ultimately, these novel optimization techniques may provide a one-stop solution for the engineering and application of density-graded structures, including the multilevel design of the structures within manufacturing capabilities.

5. Conclusion

Density-graded cellular solids are architected materials designed to conform to various application needs. The objective of this

review was to provide a comprehensive insight into the fundamental concepts, novel fabrication methods, and some of the most promising applications of density-graded cellular solids. Recent advancements achieved in the design and development of density-graded foams and lattice structures were highlighted. Density-graded cellular solids have emerged as substitutes for regular cellular solids due to their tailorable physical and mechanical properties. Perhaps the most widely used characteristic of density-graded foams and lattice structures is their unique strength–energy absorption properties that outperform

those of single-density and conventional cellular structures. It is also evident that recent advancements in additive manufacturing technologies have transformed the applications of density-graded structures, leading to the ever-increasing growth of these structures in several engineering areas. This review focused on some of the most promising areas, wherein density-graded structures have gained considerable attention, including structures, acoustics, and biomedical engineering. The survey of the available literature on the topic also revealed that great strides have recently been made to further improve the properties of graded structures in various ways, for example, by changing the geometry and topology of such structures. The recent efforts in optimizing process–structure–property interrelationships in density-graded structures seem to be the direction that the current research efforts are directed toward. In conclusion, while it is clear that significant research work needs to be done to uncover the full potentials of density-graded structures, it is also evident that the tailorability of the properties and functionalities of graded cellular structures is the primary factor that has led to and will continue to increase the rapid growth of these structures in several areas of applied science and engineering.

Acknowledgements

This material was based upon work supported by the National Science Foundation under grant no. 2035660 (B.K.) and grant no. 2035663 (G.Y.). B.K. acknowledges the Advanced Materials and Manufacturing Institute (AMMI) at Rowan University for financial support. G.Y. acknowledges support from the National Science Foundation (award no. 1925539) and the USA Department of Defense (grant agreement nos. W911NF1410039 and W911NF1810477).

Conflict of Interest

The authors declare no conflict of interest.

Keywords

additive manufacturing, cellular solids, density gradations, foams, functionally graded

Received: May 27, 2021

Revised: August 6, 2021

Published online: August 21, 2021

- [1] M. F. Ashby, L. J. Gibson, *Cellular Solids: Structure And Properties*, Cambridge University Press, Cambridge, UK **1997**.
- [2] R. Critchley, I. Corni, J. A. Wharton, F. C. Walsh, R. Wood, K. Stokes, *Physica Status Solidi (b)*. **2013**, 250, 1963.
- [3] Z. Wang, C. Luan, G. Liao, J. Liu, X. Yao, J. Fu, *Adv. Eng. Mat.* **2020**, 22, 2000312.
- [4] H. Kolken, A. Zadpoor, *RSC. Adv.* **2017**, 5111.
- [5] N. Chan, K. Evans, *J. Mater. Sci.* **1997**, 5945.
- [6] O. Duncan, T. Shepherd, C. Moroney, L. Foster, P. Venkatraman, K. Winwood, T. Allen, A. Alderson, *Appl. Sci.* **2018**, 8, 941.
- [7] Y. Li, Z. Feng, L. Hao, L. Huang, C. Xin, Y. Wang, E. Bilotti, K. Essa, H. Zhang, Z. Li, F. Yan, T. Pijs, *Adv. Mater. Technol.* **2020**, 5, 1900981.
- [8] G. H. Loh, E. Pei, D. Harrison, M. D. Monzon, *Addit. Manuf.* **2018**, 23, 34.
- [9] H. Yu, Z. Guo, B. Li, G. Yao, *Mat. Sci. Eng. A-Struct.* **2007**, 454, 542.
- [10] S. K. Maiti, L. J. Gibson, M. F. Ashby, *Acta Metallurgica* **1984**, 32, 1963.
- [11] N. Gupta, *Mater. Lett* **2007**, 61, 979.
- [12] R. Caeti, N. Gupta, M. Porfiri, *Mater. Lett.* **2009**, 63, 1964.
- [13] K. Chittineni, *J. Eng. Mater-T ASME*. **2010**, 132, 011005.
- [14] N. Gupta, B. Brar, E. Woldesenbet, *Bull. Mater. Sci.* **2001**, 24, 219.
- [15] J. Qiao, G. Wu, *J. Mater. Sci.* **2011**, 46, 3935.
- [16] B. Satapathy, A. Das, A. Patnaik, *J. Mater. Sci.* **2011**, 46, 1963.
- [17] M. Doddamani, V. Kishore, *Polym. Compos.* **2015**, 36, 685.
- [18] E. Cusson, A. Akbarzadeh, D. Therriault, D. Rodrigue, *Cell. Polym.* **2019**, 38, 3.
- [19] M. Ashby, T. Evans, N. Fleck, J. Hutchinson, H. Wadley, L. Gibson, *Metal Foams: A Design Guide*, Butterworth-Heinemann, Boston, MA, USA **2009**.
- [20] X. Yang, W. Wang, L. Yan, Q. Zhang, *J. Phys D.* **2016**, 49, 505301.
- [21] S. He, Y. Zhang, G. Dai, J. Jiang, *Mater. Sci. Eng. A.* **2014**, 618, 496.
- [22] Y. Hangai, K. Takahashi, T. Utsunomiya, S. Kitahara, O. Kuwazuru, N. Yoshikawa, *Mater. Sci. Eng. A.* **2012**, 534, 716.
- [23] Y. Hangai, K. Zushida, O. Kuwazuru, N. Yoshikawa, *Mater. Trans.* **2016**, 57, 748.
- [24] A. Hassani, A. Habibolahzadeh, H. Bafti, *Mater. Des.* **2012**, 40, 510.
- [25] N. Gupta, N. Rohatgi, *Metal matrix syntactic foams: Processing, microstructure, properties and applications*, DEStech Publications, Inc, Lancaster, PA **2004**.
- [26] A. Szlancsik, B. Katona, K. Bobor, K. Májlinger, I. Orbulov, *Mater. Des.* **2015**, 83, 230.
- [27] M. Taherishargh, I. Belova, G. Murch, T. Fiedler, *Mater. Sci. Eng. A.* **2014**, 604, 127.
- [28] S. Ferreira, A. Velhinho, R. Silva, L. Rocha, *Int. J. Mater. Prod. Technol.* **2010**, 39, 122.
- [29] K. Májlinger, I. N. Orbulov, *Mater. Sci. Eng. A.* **2014**, 606, 248.
- [30] N. Movahedi, G. Murch, I. Belova, T. Fiedler, *Mater. Des.* **2019**, 168, 107652.
- [31] D. Chen, S. Kitipornchai, J. Yang, *Mater. Des.* **2018**, 140, 473.
- [32] M. Liang, Z. Li, F. Lu, X. Li, *Compos. Struct.* **2017**, 164, 170.
- [33] J. Yang, S. Wang, Y. Ding, Z. Zheng, J. Yu, *Mater. Sci. Eng. A.* **2017**, 680, 411.
- [34] H. Zhou, X. Wang, Z. Zhao, *Compos. B. Eng.* **2016**, 85, 93.
- [35] J. Fang, Y. Gao, X. An, G. Sun, J. Chen, Q. Li, *Compos. B. Eng.* **2016**, 92, 338.
- [36] M. Liang, G. Zhang, F. Lu, X. Li, *Thin-Walled Struct.* **2017**, 112, 98.
- [37] X. Liu, X. Tian, T. Lu, B. Liang, *Int. J. Mech. Sci.* **2014**, 84, 61.
- [38] Y. Duan, X. Zhao, B. Du, X. Shi, H. Zhao, B. Hou, Y. Li, *Int. J. Mech. Sci.* **2020**, 177, 105603.
- [39] B. Koohbor, S. Ravindran, A. Kidane, *Int. J. Impact. Eng.* **2021**, 150, 103820.
- [40] B. Koohbor, B. A. Kidane, *Mater. Des.* **2016**, 102, 151.
- [41] Y. Zhang, M. Lu, G. Sun, G. Li, *Compos. Struct.* **2015**, 132, 393.
- [42] Y. Hangai, N. Utsunomiya, T. Kawashima, H. Kuwazuru, O. Yoshikawa, *Mater. Sci. Eng. A.* **2015**, 639, 597.
- [43] Y. Duan, X. Zhao, Z. Liu, N. Hou, H. Liu, B. Du, B. Hou, Y. Li, *Compos. B. Eng.* **2020**, 183, 107630.
- [44] Y. Xia, C. Wu, Z. Liu, Y. Yuan, *Constr. Build Mater.* **2016**, 111, 209.
- [45] J. Liu, B. Hou, F. Lu, H. Zhao, *Int. J. Impact Eng.* **2015**, 80, 133.
- [46] C. Shen, G. Lu, T. Yu, *Int. J. Impact Eng.* **2014**, 74, 92.
- [47] C. Shen, T. Yu, G. Lu, *Int. J. Solids. Struct.* **2013**, 50, 217.
- [48] D. Karagiozova, M. Alves, *Int. J. Solids. Struct.* **2015**, 71, 323.
- [49] H. Liu, Z. Zhang, H. Liu, J. Yang, H. Lin, *Compos. B. Eng.* **2017**, 116, 76.
- [50] P. Wang, X. Wang, Z. Zheng, J. Yu, *Lat. Am. J. Solids Struct.* **2017**, 14, 1251.
- [51] J. Zheng, Q. Qin, T. Wang, *Mech. Mater.* **2016**, 94, 66.
- [52] B. Chang, Z. Zheng, Y. Zhang, K. Zhao, S. He, J. Yu, *Int. J. Impact Eng.* **2020**, 143, 103611.

- [53] B. Koohbor, A. Kidane, W. Lu, M. Sutton, *Int. J. Impact Eng.* **2016**, *91*, 170.
- [54] B. Koohbor, A. Kidane, W. Lu, *Int. J. Impact Eng.* **2016**, *98*, 62.
- [55] S. Ravindran, B. Koohbor, A. Kidane, *Int. J. Solids. Struct.* **2018**, *270*.
- [56] C. J. Shen, G. Lu, D. Ruan, T. Yu, *Int. J. Solids. Struct.* **2016**, *88*, 319.
- [57] Y. Chen, F. Chen, Z. Du, Y. Wang, H. Hua, *Compos. B. Eng.* **2015**, *69*, 484.
- [58] Y. Chen, F. Chen, W. Zhang, Z. Du, H. Hua, *Compos. B. Eng.* **2016**, *98*, 297.
- [59] H. Liu, S. Ding, B. Ng, *Compos. B. Eng.* **2019**, *172*, 516.
- [60] F. Xu, X. Zhang, H. Zhang, *Eng. Struct.* **2018**, *171*, 309.
- [61] J. Zhou, Z. Guan, W. Cantwell, *Compos. Struct.* **2013**, *97*, 370.
- [62] X. Zhang, H. Zhang, *Int. J. Mech. Sci.* **2013**, *68*, 199.
- [63] A. Pollien, Y. Conde, L. Pambaguian, A. Mortensen, *Mater. Sci. Eng. A.* **2005**, *404*, 9.
- [64] E. Wang, N. Gardner, A. Shukla, *Int. J. Solids. Struct.* **2009**, *46*, 3492.
- [65] G. Sun, E. Wang, H. Wang, Z. Xiao, *Mater. Des.* **2018**, *160*, 1117.
- [66] S. Li, Z. Wang, G. Wu, L. Zhao, X. Li, *Compos. Part A Appl. Sci. Manuf.* **2014**, *56*, 262.
- [67] X. Zhang, M. Leary, H. Tang, T. Song, M. Qian, *Curr. Opin. Solid State Mater. Sci.* **2018**, *22*, 75.
- [68] M. Helou, S. Kara, *Int. J. Comput. Integr. Manuf.* **2018**, *31*, 243, <https://doi.org/10.1080/0951192X.2017.1407456>.
- [69] W. Tao, M. C. Leu, *International Symposium on Flexible Automation (ISFA)*, Cleveland, OH **2016**, pp. 325–332.
- [70] S. Park, D. Rosen, C. E. Duty, in *International Solid Freeform Fabrication Symposium - An Additive Manufacturing Conference*. Texas **2014**.
- [71] L. Gibson, M. Ashby, B. Harley, *Cellular Materials In Nature And Medicine*, Cambridge University Press, Cambridge, UK **2010**.
- [72] O. Abdelaal, S. M. H. Darwish, *Int. J. Innov. Res. Sci. Eng. Technol.* **2012**, *2*, 218.
- [73] Q. Zhou, *Engineering Plasticity and Impact Dynamics.* **2001**, 97.
- [74] M. Bici, S. Brischetto, F. Campana, C. Ferro, C. Seclì, S. Varetto, P. Maggiore, A. Mazza, *Procedia CIRP.* **2018**, *67*, 215.
- [75] I. Ivañez, L. Fernandez-Cañadas, S. Sanchez-Saez, *Compos. Struct.* **2017**, *174*, 123.
- [76] J. Harris, R. Winter, G. McShane, *Int. J. Impact Eng.* **2017**, *104*, 177.
- [77] J. Banhart, H. Seeliger, *Adv. Eng. Mater.* **2008**, *10*, 793.
- [78] A. Zargarian, M. Esfahanian, J. Kadkhodapour, D. Zamani, *Theor. Appl. Fract. Mech.* **2019**, *100*, 225.
- [79] Q. Xia, M. Wang, T. Shi, *Struct. Multidiscipl. Optim.* **2013**, *47*, 687.
- [80] I. Echeta, X. Feng, B. Dutton, R. Leach, S. Piano, *Int. J. Adv. Manuf. Technol.* **2020**, *106*, 2649.
- [81] C. Yan, L. Hao, A. Hussein, S. Bubb, P. Young, D. Raymont, *J. Mater. Process. Technol.* **2014**, *214*, 856.
- [82] C. Yan, L. Hao, A. Hussein, D. Raymont, *Int. J. Mach. Tools Manuf.* **2012**, *62*, 32.
- [83] X. Shi, W. Liao, P. Li, C. Zhang, T. Liu, C. Wang, J. Wu, *Adv. Eng. Mater.* **2020**, *22*, 2000453.
- [84] S. Yu, J. Sun, J. Bai, *Mater. Des.* **2019**, *182*, 108021.
- [85] O. Al-Ketan, D. Lee, R. Rowshan, R. Al-Rub, *J. Mech. Behav. Biomed. Mater.* **2020**, *102*, 103520.
- [86] C. Han, Y. Li, Q. Wang, S. Wen, Q. Wei, C. Yan, L. Hao, J. Liu, Y. Shi, *J. Mech. Behav. Biomed. Mater.* **2018**, *80*, 119.
- [87] F. Liu, Z. Mao, P. Zhang, D. Zhang, J. Jiang, Z. Ma, *Mater. Des.* **2018**, *160*, 849.
- [88] M. Afshar, A. Anaraki, H. Montazerian, *Mater. Sci. Eng. C.* **2018**, *92*, 254.
- [89] D. Qi, Q. Lu, C. He, Y. Li, W. Wu, D. Xiao, *Extreme Mech. Lett.* **2019**, *32*, 100568.
- [90] X. Wu, Y. Su, J. Shi, *Compos. Struct.* **2020**, *247*, 112451.
- [91] X. Jin, Z. Wang, J. Ning, G. Xiao, E. Liu, X. Shu, *Compos. B. Eng.* **2016**, *106*, 206.
- [92] N. Novak, M. Borovinšek, M. Vesenjok, M. Wormse, C. Körner, S. Tanaka, K. Hokamoto, Z. Ren, *Phys. Status Solidi B.* **2018**, *256*, 1800040, <https://doi.org/10.1002/pssb.201800040>.
- [93] R. Hedayati, A. Güven, S. van der Zwaag, *Appl. Phys. Lett.* **2021**, *118*, 141904.
- [94] J. Yao, R. Sun, F. Scarpa, C. Remillat, Y. Gao, Y. Su, *Compos. Struct.* **2021**, *261*, 113313.
- [95] J. Plocher, A. Panesar, *Mater. Des.* **2019**, *183*, 108164.
- [96] M. Schenk, S. Guest, *Origami* **2011**, pp. 291–304.
- [97] L. Yuan, H. Dai, J. Song, J. Ma, Y. Chen, *Mater. Des.* **2020**, *189*, 108494.
- [98] S. Callens, A. Zadpoor, *Mater. Today.* **2018**, *21*, 241.
- [99] Y. Hou, R. Neville, F. Scarpa, C. Remillat, B. Gu, M. Ruzzene, *Compos. B. Eng.* **2014**, *59*, 33.
- [100] F. Habib, P. Iovenitti, S. Masood, M. Nikzad, *Virtual Phys. Prototyp.* **2017**, *12*, 1.
- [101] W. Grunsvén, E. Hernández-Nava, G. Reilly, R. Goodall, S. Robert, *Metals.* **2014**, *4*, 401.
- [102] S. Galehdari, M. Kadkhodayan, S. Hadidi-Moud, *Int. J. Crashworthiness.* **2015**, *20*, 387.
- [103] A. Ajdari, H. Nayeb-Hashemi, A. Vaziri, *Int. J. Solids. Struct.* **2011**, *48*, 506.
- [104] S. Bates, I. Farrow, R. Trask, *Mater. Des.* **2019**, *162*, 130.
- [105] A. Brothers, D. Dunand, *Mater. Sci. Eng. A.* **2008**, *489*, 439.
- [106] M. Khan, T. Baig, S. Mirza, *Mater. Sci. Eng. A.* **2012**, *539*, 135.
- [107] L. Yang, R. Mertens, M. Ferrucci, C. Yan, Y. Shi, S. Yang, *Mater. Des.* **2019**, *162*, 394.
- [108] Y. Tao, S. Duan, W. Wen, Y. Pei, D. Fang, *Compos. B. Eng.* **2017**, *118*, 33.
- [109] S. Kumar, J. Ubaid, R. Abishera, A. Schiffer, V. S. Deshpande, *ACS Appl. Mater. Interface.* **2019**, *11*, 42549.
- [110] P. Gonzalez, E. Schwarzer, U. Scheithauer, N. Kooijmans, T. Moritz, *J. Vis. Exp.* **2019**, *143*, e57943.
- [111] T. Liu, S. Guessasma, J. Zhu, W. Zhang, S. Belhabib, *Eur. Polym. J.* **2018**, *108*, 199.
- [112] V. Tambrallimath, R. Keshavamurthy, D. Saravanabavan, P. Koppad, G. Kumar, *Compos. Commun.* **2019**, *15*, 129.
- [113] O. Mohamed, S. Masood, J. Bhowmik, *Adv. Manuf.* **2015**, *3*, 42.
- [114] L. Safai, J. Cuellar, G. Smit, A. Zadpoor, *Adv. Manuf.* **2019**, *28*, 87.
- [115] O. Rahman, B. Koohbor, *Compos. Part C* **2020**, *3*, 100052.
- [116] R. Duraibabu, R. Prithvirajan, M. Sugavaneswaran, G. Arumaikkannu, *Mater. Today.* **2020**, *24*, 1035.
- [117] C. Bae, A. Diggs, A. Ramachandran, *Addit. Manuf.* **2018**, *6*, 181.
- [118] S. Sing, C. Tey, J. Tan, S. Huang, W. Yeong, *3D Printing Of Metals In Rapid Prototyping Of Biomaterials: Techniques In Additive Manufacturing*, Elsevier, Cambridge, MA, USA **2020**.
- [119] J. Najmon, S. Raeisi, A. Tovar, *Review Of Additive Manufacturing Technologies And Applications In The Aerospace Industry*, Elsevier, Cambridge, MA, USA **2019**.
- [120] K. Deshmukh, A. Muzaffar, T. Kovářka, T. Křenek, M. Ahamed, S. Pasha, *Fundamentals And Applications Of 3D And 4D Printing Of Polymers: Challenges In Polymer Processing And Prospects Of Future Research*, Elsevier, Cambridge, MA, USA **2019**.
- [121] C. Zhang, F. Chen, Z. Huang, M. Jia, G. Chen, Y. Ye, Y. Lin, W. Liu, B. Chen, Q. Shen, L. Zhang, E. Lavernia, *Mater. Sci. Eng. A.* **2019**, *764*, 138209.
- [122] I. Maskery, N. Aboulkhair, A. Aremu, C. Tuck, I. Ashcroft, R. Wildman, R. Hague, *Mater. Sci. Eng. A.* **2016**, *670*, 264.
- [123] S. Choy, C. Sun, K. Leong, J. Wei, *Mater. Des.* **2017**, *131*, 112.
- [124] T. Cox, P. D'antonio, *Acoustic Absorbers And Diffusers: Theory, Design And Application*, Spon Press, Boca Raton, Florida, USA **2009**.
- [125] M. Navacerrada, P. Fernández, C. Díaz, A. Pedrero, *Appl. Acoust.* **2013**, *74*, 496.

- [126] H. Ke, Y. Donghui, H. Siyun, H. Deping, *J. Phys. D. Appl. Phys.* **2011**, *44*, 365405.
- [127] S. Mosanenzadeh, H. Naguib, C. Park, N. Atalla, *J. Mater. Sci.* **2015**, *50*, 1248.
- [128] H. Meng, Q. Ao, H. Tang, F. Xin, T. Lu, *Sci. China Technol. Sci.* **2014**, *57*, 2096.
- [129] H. Meng, F. Xin, T. Lu, *J. Vib. Acoust.* **2014**, *136*, 061007.
- [130] W. Chen, S. Liu, L. Tong, S. Li, *Theor. Appl. Mech. Lett.* **2016**, *6*, 42.
- [131] N. Jingfeng, *J. Vib. Control.* **2016**, *22*, 2861.
- [132] M. Lewińska, J. van Dommelen, V. Kouznetsova, M. Geers, *J. Sound. Vib.* **2020**, *483*, 115472.
- [133] Y. Feng, J. Qiao, L. Li, *Mater. Des.* **2020**, *193*, 108870.
- [134] S. Cummer, J. Christensen, A. Alù, *Nat. Rev. Mater.* **2016**, *1*, 16001.
- [135] A. Climente, D. Torrent, J. Sánchez-Dehesa, *Appl. Phys. Lett.* **2010**, *97*, 104103.
- [136] Y. Xie, Y. Fu, Z. Jia, J. Li, C. Shen, Y. Xu, H. Chen, S. Cummer, *Sci. Rep.* **2018**, *8*, 16188.
- [137] Y. Fu, J. Li, Y. Xie, C. Shen, Y. Xu, H. Chen, S. Cummer, *Phys. Rev. Mater.* **2018**, *2*, 105202.
- [138] A. Climente, D. Torrent, J. Sánchez-dehesa, *Appl. Phys. Lett.* **2012**, *100*, 144103.
- [139] C. Naify, T. Martin, C. Layman, M. Nicholas, A. Thangawng, D. Calvo, G. Orris, *Appl. Phys. Lett.* **2014**, *104*, 073505.
- [140] Y. Liang, L. Chen, C. Wang, I. Chang, *J. Appl. Phys.* **2014**, *115*, 244513.
- [141] Z. Gu, B. Xue-Jiang, Y. Liang, X. Li, L. Zou, J. Yin, J. Cheng, *Appl. Phys.* **2015**, *117*, 074502.
- [142] S. Tol, F. Degertekin, A. Erturk, *Appl. Phys. Lett.* **2017**, *111*, 013503.
- [143] J. Hyun, C. Park, J. Chang, W. Cho, M. Kim, *Appl. Phys. Lett.* **2020**, *116*, 234101.
- [144] Z. Li, D. Yang, S. Liu, S. Yu, M. Lu, J. Zhu, S. Zhang, M. Zhu, X. Guo, H. Wu, X. Wang, Y. Chen, *Sci. Rep.* **2017**, *7*, 42863.
- [145] Y. Ding, E. Statharas, K. Yao, M. Hong, *Appl. Phys. Lett.* **2017**, *110*, 241903.
- [146] Y. Jin, B. Djafari-Rouhani, D. Torrent, *Nanophotonics.* **2019**, *8*, 685.
- [147] B. Assouar, B. Liang, Y. Wu, Y. Li, J. Cheng, Y. Jing, *Nat. Rev. Mater.* **2018**, *3*, 460.
- [148] Y. Xie, W. Wang, H. Chen, A. Konneker, *Nat. Commun.* **2014**, *5*, 5553.
- [149] K. Tang, C. Qiu, M. Ke, J. Lu, Y. Ye, Z. Liu, *Sci. Rep.* **2014**, *4*, 6517.
- [150] G. Memoli, M. Caleap, M. Asakawa, D. Sahoo, B. Drinkwater, S. Subramanian, *Nat. Commun.* **2017**, *8*, 14608.
- [151] X. Zhu, K. Li, P. Zhang, J. Zhu, J. Zhang, C. Tian, S. Liu, *Nat. Commun.* **2016**, *7*, 1.
- [152] Y. Shen, Y. Peng, F. Cai, K. Huang, D. Zhao, C. Qiu, H. Zheng, X. Zhu, *Nat. Commun.* **2019**, *10*, 1.
- [153] H. Tang, Z. Chen, N. Tang, S. Li, Y. Shen, Y. Peng, X. Zhu, J. Zang, *Adv. Func. Mater.* **2018**, *28*, 1801127.
- [154] C. Shen, Y. Xie, J. Li, S. Cummer, Y. Jing, *Appl. Phys. Lett.* **2016**, *108*, 223502.
- [155] Y. Li, C. Shen, Y. Xie, J. Li, W. Wang, S. Cummer, Y. Jing, *Phys. Rev. Lett.* **2017**, *119*, 035501.
- [156] J. Xia, X. Zhang, H. Sun, S. Yuan, J. Qian, Y. Ge, *Phys. Rev. Appl.* **2018**, *10*, 014016.
- [157] X. Zhu, H. Ramezani, C. Shi, J. Zhu, X. Zhang, *Phys. Rev. X* **2014**, *4*, 031042.
- [158] T. Liu, X. Zhu, F. Chen, S. Liang, J. Zhu, *Phys. Rev. Lett.* **2018**, *120*, 124502.
- [159] K. Melde, A. Mark, T. Qiu, P. Fischer, *Nature.* **2016**, *537*, 518.
- [160] Y. Xie, C. Shen, W. Wang, J. Li, D. Suo, B. Popa, Y. Jing, S. Cummer, *Sci. Rep.* **2016**, *6*, 35437.
- [161] Y. Zhu, J. Hu, X. Fan, J. Yang, B. Liang, X. Zhu, J. Cheng, *Nat. Commun.* **2018**, *9*, 1.
- [162] Y. Peng, Y. Shen, Z. Geng, P. Li, J. Zhu, X. Zhu, *Sci. Bull.* **2020**, *65*, 1022.
- [163] L. Cox, K. Melde, A. Croxford, P. Fischer, B. Drinkwater, *Phys. Rev. Appl.* **2019**, *12*, 064055.
- [164] Z. Ma, A. Holle, *Adv. Mater.* **2020**, *32*, 1904181.
- [165] Y. Gu, C. Chen, J. Rufo, C. Shen, Z. Wang, P. Huang, H. Fu, P. Zhang, S. Cummer, Z. Tian, T. Huang, *ACS Nano.* **2020**, *14*, 14635.
- [166] M. Yang, S. Chen, C. Fu, P. Sheng, *Mater. Horiz.* **2017**, *4*, 673.
- [167] C. Zhang, X. Hu, *Phys. Rev. Appl.* **2016**, *6*, 064025.
- [168] C. Shen, S. Cummer, *Rev. Appl.* **2018**, *9*, 054009.
- [169] X. Peng, J. Ji, Y. Jing, *J. Acoust. Soc. Am.* **2018**, *144*, EL255.
- [170] S. Huang, Z. Zhou, D. Li, T. Liu, X. Wang, J. Zhu, Y. Li, *Sci. Bull.* **2020**, *65*, 373.
- [171] K. Melde, E. Choi, Z. Wu, S. Palagi, T. Qiu, P. Fischer, *Adv. Mater.* **2018**, *30*, 1704507.
- [172] C. Shi, M. Dubois, Y. Wang, X. Zhang, P. Sheng, in *Proc. Natl. Acad. Sci. U S A.* **2017**, Vol. *114*, pp. 7250–7253.
- [173] X. Jiang, B. Liang, J. Cheng, C. Qiu, *Adv. Mater.* **2018**, *30*, 1800257.
- [174] S. Jiménez-Gambín, N. Jiménez, J. Benlloch, F. Camarena, *Phys. Rev. Appl.* **2019**, *12*, 014016.
- [175] J. Lowen, J. Leach, *Adv. Funct. Mater.* **2020**, *30*, 1909089.
- [176] T. Nie, L. Xue, M. Ge, H. Ma, J. Zhang, *Mater. Lett.* **2016**, *176*, 25.
- [177] A. Maggi, L. Hanqing, J. Greer, *Acta Biomater.* **2017**, *63*, 294.
- [178] J. Warner, A. Gillies, H. Hwang, H. Zhang, R. Lieber, S. Chen, *J. Mech. Behav. Biomed.* **2017**, *76*, 145.
- [179] Y. Jiang, Z. Liu, N. Matsuhisa, D. Qi, W. Leow, H. Yang, J. Yu, G. Chen, Y. Liu, C. Wan, Z. Liu, X. Chen, *Adv. Mater.* **2018**, *30*, 1706589.
- [180] Z. Lu, Y. Tang, Z. Zhu, J. Wei, W. Li, H. Xia, Y. Jiang, Z. Liu, Y. Luo, X. Ge, Y. Zhang, R. Wang, W. Zhang, X. Loh, X. Chen, *Adv. Mater.* **2018**, *30*, 1805468.
- [181] H. Kolken, S. Janbaz, S. Leeftang, K. Lietaert, H. Weinans, A. Zadpoor, *Mater. Horiz.* **2018**, *5*, 28.
- [182] M. Qwamizadeh, P. Liu, Z. Zhang, K. Zhou, Y. Zhang, *J. Appl. Mech.* **2016**, *83*, 051009.
- [183] H. Cui, W. Zhu, M. Nowicki, X. Zhou, A. Khademhosseini, L. Zhang, *Adv. Healthc. Mater.* **2016**, *5*, 2174.
- [184] H. Niknam, A. Akbarzadeh, *Mater. Des.* **2020**, *196*, 109129.
- [185] M. Vargas, *Planar Metamaterial Based Microwave Sensor Arrays For Biomedical Analysis And Treatment.* Springer Science & Business Media, Springer, New York, NY, USA **2014**.
- [186] I. Al-Naib, *IEEE J. Sel. Top. Quantum Electron.* **2016**, *23*, 1.
- [187] K. Amireddy, K. Balasubramaniam, P. Rajagopal, *Sci. Rep.* **2017**, *7*, 1.
- [188] K. Amireddy, K. Balasubramaniam, P. Rajagopal, *Appl. Phys. Lett.* **2018**, *113*, 124102.
- [189] S. Chen, J. Xu, N. Fang, Y. Jing, *Phys. Rev. X* **2014**, *4*, 041033.
- [190] M. Thieme, K. Wieters, F. Bergner, D. Scharnweber, H. Worch, J. Ndop, T. Kim, W. Grill, *J. Mater. Sci. Mater. Med.* **2001**, *12*, 225.
- [191] M. Suk, S. Choi, J. Kim, Y. Kim, Y. Kwon, *Met. Mater. Int.* **2003**, *9*, 599.
- [192] A. Sadollah, A. Bahreininejad, *J. Mech. Biomed. Mater.* **2011**, *4*, 1384.
- [193] H. Hedia, N. Mahmoud, *Biomed. Mater. Eng.* **2004**, *14*, 133.
- [194] Y. Zhang, M. Sun, D. Zhang, *Acta Biomater.* **2012**, *8*, 1101.
- [195] A. Boccaccio, A. Uva, M. Fiorentino, G. Mori, G. Monno, *Plos One.* **2016**, *11*, e0146935.
- [196] A. Yokoyama, F. Watari, R. Miyao, H. Matsuno, M. Uo, T. Kawasaki, T. Kohgo, M. Omori, T. Hirai, *Key Eng. Mater.* **2000**, *192*, 445.
- [197] M. Mehrali, F. Shirazi, M. Mehrali, H. Metselaar, N. Kadri, N. Osman, *J. Biomed. Mater. Res. A.* **2013**, *3046*.
- [198] B. Rego, M. Sacks, *J. Appl. Biomech.* **2017**, *54*, 88.
- [199] H. Schliephake, F. Neukam, D. Klosa, *Int. J. Oral Maxillofac. Surg.* **1991**, *20*, 53.

- [200] M. Rueda, L. Cui, M. Gilchrist, *Mater. Des.* **2009**, 30, 3405.
 [201] L. Cui, M. Rueda, M. Gilchrist, *Mater. Des.* **2009**, 30, 3414.
 [202] Y. Shimazaki, S. Nozu, T. Inoue, *Polym. Test.* **2016**, 54, 98.
 [203] W. Zhang, S. Sun, *Int. J. Numer. Methods Eng.* **2006**, 68, 993.
 [204] Y. Zhang, L. Gao, M. Xiao, *Comput. Struct.* **2020**, 230, 106197.
 [205] U. SImsek, C. E. Gayir, G. Kiziltas, P. Sendur, *Int. J., Adv. Manuf. Technol.* **2020**, 111, 1361.
 [206] N. Jawahar, R. Subhaa, *J. Manuf. Syst.* **2017**, 44, 115.
 [207] A. Bessa, P. Glowacki, M. Houlder, *Adv. Mater.* **2019**, 31, 1904845.
 [208] J. K. Wilt, C. Yang, G. X. Gu, *Adv. Eng. Mater.* **2020**, 22, 1901266.
 [209] A. Cramer, V. Challis, A. Roberts, *Struct. Multidiscip. Optim.* **2016**, 53, 489.
 [210] L. Cheng, J. Bai, A. To, *Comput. Methods in Appl. Mech. Eng.* **2019**, 344, 334.
 [211] A. Casalotti, F. D'Annibale, G. Rosi, *Compos. Struct.* **2020**, 252, 112608.
 [212] Y. Wang, J. Groen, O. Sigmund, *Extrem. Mech. Lett.* **2019**, 29, 100447.
 [213] J. Berger, H. Wadley, R. McMeeking, *Nature.* **2017**, 543, 533.
 [214] S. Das, A. Sutradhar, *Mater. Des.* **2020**, 193, 108775.
 [215] D. Li, W. Liao, N. Dai, G. Dong, Y. Tang, Y. Xie, *Comput. Aided Des.* **2018**, 104, 87.
 [216] S. Daynes, S. Feih, W. Lu, J. Wei, *Mater. Des.* **2017**, 127, 215.
 [217] A. Panesar, M. Abdi, D. Hickman, I. Ashcroft, *Addit. Manuf.* **2018**, 19, 81.
 [218] K. Uddin, G. Youssef, M. Trkov, H. Seyyedhosseinzadeh, B. Koozbor, *J. Biomech.* **2020**, 109, 109950.
 [219] P. Zhang, J. Toman, Y. Yu, E. Biyikli, M. Kirca, M. Chmielus, A. To, *J. Manuf. Sci. Eng.* **2015**, 137, 2015.
 [220] L. Cheng, P. Zhang, E. Biyikli, J. Bai, *Rapid Prototyp. J.* **2017**, 23, 660.
 [221] R. Gorgularslan, U. Gandhi, Y. Song, S. Choi, *Rapid Prototyp. J.* **2017**, 23, 305.
 [222] J. Plocher, A. Panesar, *JOM.* **2020**, 72, 1292.
 [223] J. Plocher, A. Panesar, *Addit. Manuf.* **2020**, 33, 101171.



Oyindamola Rahman is a recent graduate of the Mechanical Engineering M.Sc. degree program of Rowan University. She received her B.Sc. in mechanical engineering from the University of Ilorin. Her research focuses on the optimization of load bearing and impact energy absorption capacities of density-graded honeycomb structures.



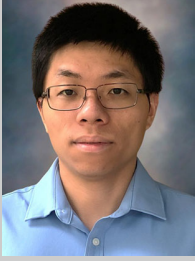
Kazi Zahir Uddin is a graduate research fellow at Rowan University. He received his bachelor of science degree in mechanical engineering from Chittagong University of Engineering and Technology. His research focus is on fabrication and multiscale characterization of multifunctional material.



Jeeva Muthulingam is a Ph.D. student at Rowan University. He received his M.Tech. in mechanical systems and design at the Indian Institute of Technology, Kharagpur. His current research focuses on micromechanics of composites and cold spray processing of polymers and polymer composites.



George Youssef is a professor of mechanical engineering at San Diego State University. He received his Ph.D. in mechanical engineering at the University of California, Los Angeles. His research focuses on experimental solid mechanics of polymers, composites, and smart materials.



Chen Shen is currently an assistant professor in the Department of Mechanical Engineering at Rowan University. He received his B.S. at Nanjing University in 2012 and Ph.D. at North Carolina State University in 2016. His research focuses on acoustic/elastic metamaterials, wave propagation, and mechanics of advanced materials.



Behrad Koohbor is an assistant professor of mechanical engineering at Rowan University. He received his Ph.D. from the University of South Carolina. He joined Rowan University in 2019 after completing a postdoctoral research fellowship at the University of Illinois at Urbana-Champaign. His current research focuses on the fabrication, multiscale characterization, and optimization of novel functionally graded structures.